

Compute Allocation in Evolutionary Search: From Depth–Breadth to Multi-Armed Bandits

Sixue Xing^{*1} Haoyu He^{*2} Kerui Wu^{*3}
Zhuo Yang⁴ Haozheng Luo⁵ Tianfan Fu^{6,7} Aarthy Nagarajan¹

¹University of Notre Dame ²Northeastern University ³University of Massachusetts Amherst
⁴Southeast University ⁵Northwestern University ⁶Nanjing University
⁷Shanghai Artificial Intelligence Laboratory

Abstract

LLM-guided evolutionary search (Evolve systems) has reached state-of-the-art results on mathematical and combinatorial tasks, yet most existing systems report only the best of many runs and leave the run-to-run distribution undocumented. We ask how a fixed budget of LLM calls should be allocated, and how reliably a single run reaches the reported numbers. Sweeping the depth–breadth grid over five models and three tasks, we identify two empirical regularities: a fitness–compute envelope along which capability ordering largely collapses on effective FLOPs, and a bilinear depth–breadth fit with task-specific interaction; both are gated by model–task capability. Motivated by these regularities, we propose BaSE (Bandit-based Self-Evolving), a multi-armed bandit that allocates LLM calls across parallel trajectories. Without changing the model, prompt, or evaluator, BaSE improves mean fitness by 12.3% over the strongest island-protocol baseline across 8 (model, task) cells, with the largest gains on high-variance settings: a reliability gain from allocation alone. The code is available at: <https://github.com/keruiwu/self-evolving-allocation>.

1 Introduction

Large language models are increasingly used as mutation engines for evolutionary search: given a candidate program, a frozen LLM proposes variants; a deterministic evaluator scores them; the best variant seeds the next round (Romera-Paredes et al., 2024; Novikov et al., 2025). The resulting *Evolve* systems (Lange et al., 2025; Wang et al., 2025; Assumpção et al., 2025; Cemri et al., 2026) have produced state-of-the-art results across mathematical discovery, combinatorial optimization, and algorithm design. However, the headline numbers *Evolve* systems report are systematically incomparable: FunSearch reports a 4-of-140 hit rate

* Co-first authors.

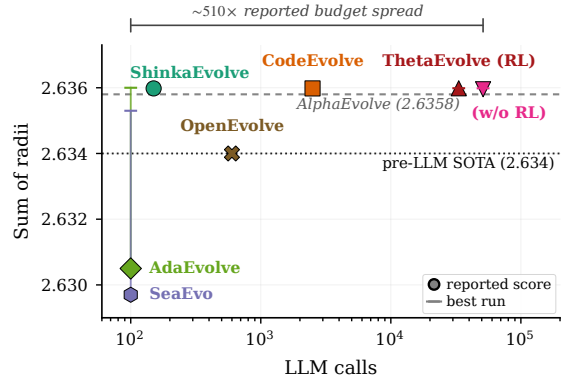


Figure 1: Cost–performance frontier on $n=26$ Circle Packing (CP).

(Romera-Paredes et al., 2024); CodeEvolve displays “only the best” (Assumpção et al., 2025); AlphaEvolve reports a single number on the $n=26$ Circle Packing benchmark (Novikov et al., 2025). Reported per-run cost spans more than two orders of magnitude, from ~ 150 LLM calls in ShinkaEvolve (Lange et al., 2025) to the 204,800 candidates ThetaEvolve processes in a single run (Wang et al., 2025). Figure 1 plots these reports on a common axis: each point is a single hand-picked configuration, and the dominant convention is to report only the best of an unspecified number of runs. Few systems report the run-to-run distribution behind these headline numbers. Combined with the order-of-magnitude variation in reported computational cost, this makes the numbers an unreliable guide to single-run performance under realistic deployment settings: existing reports characterize what is achievable on a favorable run, not what a practitioner should expect at a finite computational cost.

The expected performance is shaped by multiple design choices. A stronger base model can generate better mutations; a more informative prompt can guide the search toward more useful edits; and, importantly, allocation determines how the evolutionary process balances exploration and exploitation.

This allocation effect is orthogonal to model and prompt quality, and remains meaningful once the model, prompt, and evaluator are fixed. Better allocation can improve expected outcomes by avoiding both premature commitment to weak trajectories and excessive breadth without refinement.

While **Evolve* systems are often described as iterative loops that continue until progress saturates, practical deployments must operate under explicit resource constraints, such as a fixed number of model calls, a limited compute allocation, or a bounded experimental campaign. This motivates a controlled study of expected performance and reliability in LLM-guided evolutionary search. We adopt the fixed-budget perspective (Jansen and Zarges, 2012) from classical evolutionary computation and bring it to LLM-guided evolution. To this end, we conduct the first empirical study of cost allocation in LLM-guided evolutionary search, characterizing how a fixed number of LLM call should be spent, and use the resulting picture to ask whether allocation can be precomputed offline or must be discovered online. In summary, our contributions are listed below:

1. Proposed the first systematic empirical measurement of fixed-budget allocation between exploration and exploitation in LLM-guided evolutionary search.
2. Identified two regularities: (i) a performance–compute envelope of attainable fitness against effective FLOPs, along which capability ordering largely collapses among capable models; and (ii) a parametric depth–breadth regularity characterizing each model–task cell.
3. Designed an adaptive bandit allocator (BaSE) over parallel evolutionary trajectories, improving best mean fitness by **12.3%** on average over the strongest island-protocol baseline across 8 (model, task) cells — this is not a model improvement, nor a prompt improvement, but an allocation improvement.

2 Related Work

LLM-Guided Evolutionary Search. FunSearch (Romera-Paredes et al., 2024) introduced LLMs as mutation operators in evolutionary program synthesis, and AlphaEvolve (Novikov et al., 2025) scaled the paradigm to state-of-the-art results. **Evolve* variants vary individual axes — sample efficiency

(Lange et al., 2025), test-time RL (Wang et al., 2025), open-source islands — with adjacent work on code, architectures, and prompts (Lehman et al., 2022; Chen et al., 2023; Yang et al., 2023); all leave population size and generation count hand-set. ThetaEvolve only notes qualitatively that small databases progress faster early but large ones win at scale (Wang et al., 2025), and Population-Evolve sweeps population size without holding total budget fixed (Zhang et al., 2025). Adjacent allocation work routes compute between islands (Cemri et al., 2026), compares evolution to best-of-N and sequential revision (Lee et al., 2025), or focuses on parent sampling (Novikov et al., 2025; Lange et al., 2025) and combination operators (Lange et al., 2023; Meyerson et al., 2024). The closest precedent, ShinkaEvolve (Lange et al., 2025), uses a bandit to ensemble *models* at the final phase; we instead target the within-run depth–breadth split.

Compute Allocation. Inference-scaling work allocates test-time compute (Snell et al., 2024; Brown et al., 2024; Wu et al., 2024; Chen et al., 2024), with breadth-vs-depth studies on single-query reasoning and tree search (Sharma and Chopra, 2025; Wen et al., 2025; Inoue et al., 2025; Miyamoto et al., 2026) reporting empirical, regime-dependent curves; none targets population-based evolution with parent-conditioned mutation. Our online allocator draws on multi-armed bandits (Auer et al., 2002a; Lattimore and Szepesvári, 2020) and fixed-budget best-arm identification (Audibert and Bubeck, 2010; Karnin et al., 2013), with precedents in hyperparameter search (Li et al., 2018), prompt selection (Shi et al., 2024), MCTS expansion (Inoue et al., 2025), island routing (Cemri et al., 2026), and code repair (Tang et al., 2024), all of which *assume* adaptive allocation helps. Classical EA contributes optimal-population-under-fixed-compute analyses (Nakano et al., 1994; Briesch et al., 2023), offspring-size theory (Jansen et al., 2005; Doerr and Künnemann, 2015; Gießen and Witt, 2017; Badkobeh et al., 2014), and the fixed-budget framing (Jansen and Zarges, 2012, 2014); all assume random mutation, whereas LLM mutation carries code priors and discrete attractors that break i.i.d. mean-field assumptions, so we characterize the surface empirically.

3 Problem Formulation

Self-Evolving. In high level, we formulate self-evolution as an iterative optimization process under

a fixed inference budget of C LLM calls. Specifically, as described in [Algorithm 1](#), a Self-Evolve system repeatedly generates a candidate response, evaluates its quality, and refines the proposed solution based on historical response-evaluation pairs.

Algorithm 1 Self-Evolving Process

Require: Task q , base LLM f , prompt generator h , budget (number of LLM calls) C

- 1: **for** $c = 1, \dots, C$ **do**
- 2: prompt $\leftarrow h\left(q, \left(\text{response}^{(j)}, \text{score}^{(j)}\right)_{j \in [c]}\right)$
- 3: response^(c+1) $\leftarrow f(\text{prompt})$
- 4: score^(c+1) $\leftarrow \text{Eval}\left(q, \text{response}^{(c+1)}\right)$
- 5: **end for**
- 6: $j^* \leftarrow \arg \max_{j \in [C]} \text{score}^{(j)}$
- 7: **return** response^(j*)

The key design question in this process is the *parent sampling protocol* described in [Line 2](#) of [Algorithm 1](#): how should the system select and reuse historical responses when constructing the next prompt? This choice determines how the evolutionary process balances exploitation of high-performing solutions with exploration of diverse alternatives. In this work, we explored two representative protocols: *greedy* and *island*:

Greedy Protocol. At each generation, greedy protocol selects the current best-scoring response as the parent and generates N children from it in parallel. Equivalently, it spends N LLM calls per generation refining the best solution found so far.

Island Protocol. The island protocol originates in classical evolutionary computation ([Tanese, 1989](#)) and was brought into LLM-guided evolutionary search by FunSearch ([Romera-Paredes et al., 2024](#)), later adopted by many Evolve-style systems; it maintains a population database partitioned into multiple islands. At each generation, it first selects an island according to a MAP-Elites-style coverage rule ([Mouret and Clune, 2015](#)), and then samples a parent uniformly from that island.

The Depth–Breadth Allocation Problem. Under the greedy protocol, a run of budget C is fully specified by how that budget is split: T generations of N children each, so that:

$$C = T \cdot N,$$

The two ends of this split are familiar limits: $T=1$ spends the whole budget on a single generation of parallel samples (best-of- N), whereas $T=C$ refines one trajectory for C sequential steps. Let

$V(C, T)$ be the expected best fitness of a run at budget C and depth T . Holding the evaluator, prompt template, base model, and initial program fixed, the split is the only remaining degree of freedom, and we seek the *compute-optimal depth*

$$\begin{aligned} T^*(C) &= \arg \max_T V(C, T), \\ V_{\max}(C) &= \max_T V(C, T). \end{aligned} \tag{1}$$

the question we take up in [Section 5](#) is how $V(C, T)$ varies with allocation.

4 Experiment Setup

Tasks. We evaluate three geometric optimization tasks drawn from AlphaEvolve and shipped with the OpenEvolve example suite: **Circle Packing** (CP, $n=26$), **MinMaxDist** (MMD, $n=16$), and **Heilbronn Triangle** (HT, $n=11$). For each task we use the OpenEvolve evaluator and initial-program files verbatim, and normalize raw objectives by the best published construction so that $\text{FITNESS}=1.0$ matches the state-of-the-art. Full problem statements and normalizers are in [Appendix B](#).

Models. We sweep the open-weight Qwen3 family at four sizes: 1.7B, 4B, 8B, and 14B, all with thinking mode enabled and Llama-3.1-8B (Llama), temperature 0.6, top- p 0.95. Inference is served by vLLM v0.18 with `-quantization fp8, -max-model-len = 40960, -max-num-seqs = 16`. The vllm server runs with up to 16 in-flight parallel LLM calls on H100 GPU.

Bandits Algorithms. In [Section 6](#), we explore the impact of different runs against fitness score performance and employ Multi-Armed Bandits (MAB) for adaptive trajectory allocation. We implement three classic MAB algorithms, namely, Upper Confidence Bound (UCB) ([Auer et al., 2002b](#)), Exponential-weight algorithm for Exploration and Exploitation with high Probability (EXP3.P) ([Auer et al., 2002b](#)), and Thompson Sampling (Thompson) ([Thompson, 1933](#); [Agrawal and Goyal, 2012](#)), as well as one naive random baseline¹, sampling parent from evolve trajectories.

Parameters. We sweep greedy on Qwen3 8B/14B and Llama at $C \in \{8, \dots, 512\}$ with $T \in \{1, 2, 4, \dots, C\}$ (smaller Qwen3 1.7B/4B capped

¹We emphasize that random is a MAB algorithm baseline that chooses which evolving trajectory to pull instead of choosing parent inside the evolving process.

at $C=128$), 10 seeds per cell; $T=1$ recovers best-of- N , $T=C$ is pure sequential. Island protocols (OpenEvolve, CodeEvolve, ShinkaEvolve) run at $C=512$ on the same three models. For each (model, task) cell, Bandit and all protocols run end-to-end 10 times with independent LLM seeds. We report stratified bootstrap standard errors and 95% CIs over the 1000 resamples, following the reliable evaluation protocol of Agarwal et al. (2022).

Post-hoc FLOPs accounting. Counting LLM calls (C) is not a fair cost axis across models or protocols: different model sizes and different prefix-cache hit rates (greedy reuses one parent prefix across N siblings; island rewrites the prompt per call) consume substantially different FLOPs at the same C . Following Hoffmann et al. (2022), we charge each LLM call:

$$\text{FLOPs}_{\text{call}} = 2 P_{\text{active}} (p_{\text{prompt}} - p_{\text{cached}} + p_{\text{out}}),$$

where P_{active} is the active parameter count and $p_{\text{prompt}}, p_{\text{cached}}, p_{\text{out}}$ are the prompt, prefix-cached, and completion token counts. Per-run FLOPs sum over all calls. See Appendix A for full definitions. FLOPs/ C varies by under 15% across T at fixed C within each model ($R^2 \geq 0.94$, pooled linear fit; Figure 3, top row), so we use C within models and effective FLOPs across models.

5 Depth–Breadth Allocation

We do greedy runs, whose budget decomposes cleanly as $C=T \cdot N$, making depth–breadth allocation the only remaining degree of freedom. We analyze the full (C, T) sweep in two steps: Section 5.1 asks *how much* fitness a budget buys, on a cost axis comparable across model sizes. Section 5.2 asks *how* the budget should be split, and fits a parametric regularity to the depth–breadth surface.

5.1 The Fitness–Compute Envelope

At each budget we summarize the sweep by the best fitness $V_{\text{max}}(C)$, the highest fitness achieved across all tested depth–breadth allocations at that compute level, following the compute–performance envelope convention of Hoffmann et al. (2022), and study how it scales with effective FLOPs. We further measure compute in effective FLOPs for comparing this envelope across models (Section 4) and study V_{max} (best in-sweep allocation) on that axis. Figure 2 reports V_{max} and the best-of- N baseline against this axis. For every model V_{max} rises

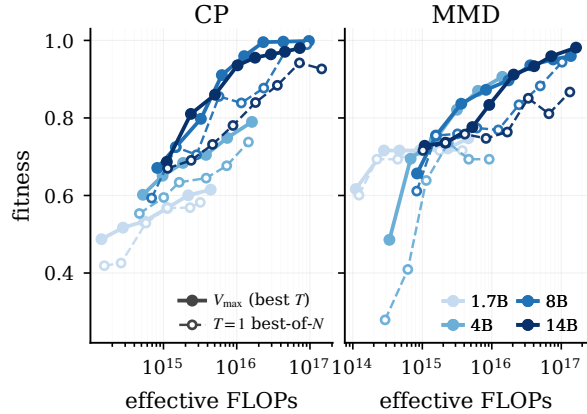


Figure 2: Fitness versus effective FLOPs. Solid lines report V_{max} over swept depth–breadth allocations; dashed lines report the pure best-of- N baseline ($T = 1$). Vertical gap between solid and dashed curves is the gain of ‘evolving’ from using evaluator feedback across generations rather than spending the full budget on one generation of parallel samples.

smoothly and monotonically with compute compute envelope. This is a clean envelope with no phase transitions or reversals.

Capability ordering collapsing. At equal LLM call count, larger models lead, but the lead is not free: a larger model spends proportionally more FLOPs per call. Re-priced in effective FLOPs (Figure 2), the ordering largely dissolves: on MMD the 4B, 8B and 14B envelopes nearly coincide ($R^2 = 0.94$); on CP: 8B and 14B coincide over the sub-ceiling range ($R^2 = 0.93$). This collapse itself is gated by model–task capability (Appendix C).

Allocation improves fitness. The vertical gap between the solid envelope and the dashed best-of- N baseline in Figure 2 is the gain from multi-generation refinement. At $C=128$ it reaches up to a tenth of the normalized fitness range (+0.119 on CP 8B, +0.102 on MMD 8B); it persists on unsaturated tasks (+0.115 on MMD 14B at $C=512$) but diminishes where the task saturates (+0.016 on MMD 8B). A selection-free test confirms a real onset on MMD but no sharp threshold on CP. Allocation thus yields real but task-dependent gains, whose structure we characterize in Section 5.2.

5.2 The Depth–Breadth Regularity

The depth–breadth split determines where on the fitness landscape a run lands. Here we characterize the landscape itself.

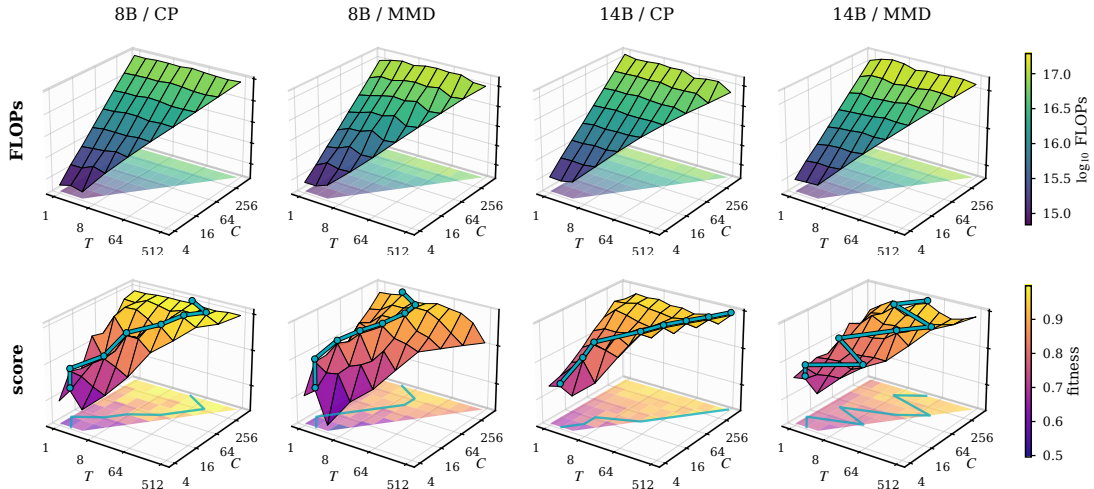


Figure 3: Full (C, T) surfaces for the $C=512$ sweeps. Top: effective FLOPs; bottom row: mean fitness. The FLOPs surfaces are nearly flat in T at fixed C , so changes along the depth axis mostly reflect allocation effects rather than hidden cost differences. The score surfaces reveal different allocation geometry: Circle Packing is depth-favored with broad plateaus, whereas MinMaxDist has an interior ridge.

Table 1: Posthoc depth–breadth gap model on sub-ceiling cells of the $C=512$ sweeps. Coefficients are for Equation (2) with natural logs. MMD has a clearly negative interaction (interior ridge) on both capable models; CP and HT sit near the corner limit ($|c| < 0.03$).

Task	Model	β_0	a	b	c	R^2
CP	8B	-0.020	-0.602	-0.496	-0.027	0.811
CP	14B	-0.561	-0.442	-0.373	0.007	0.785
MMD	8B	-0.590	-0.208	-0.290	-0.106	0.916
MMD	14B	-0.641	-0.342	-0.238	-0.057	0.869
HT	8B	0.592	-0.363	-0.168	-0.012	0.853
CP	1.7B	-0.498	-0.076	-0.088	0.001	0.724
CP	4B	-0.524	-0.190	-0.157	-0.017	0.870
MMD	4B	-0.223	-0.418	-0.248	0.024	0.732

The fitness landscape. For a practitioner with fixed budget C , choosing T is equivalent to selecting a point on the fitness surface along the budget slice of C . As Figure 3 shows, the effective-FLOPs surface (top) is approximately linear in T and remains weakly dependent on T at fixed C , so fitness differences along the depth axis reflect allocation choices rather than hidden cost variation. The fitness surface (bottom) reveals different geometries across tasks: CP shows a broad plateau where many depth allocations achieve near-equivalent fitness, whereas MMD shows an interior ridge where only a balanced depth allocation achieves the highest in-sweep fitness. The same protocol and budget range thus produce qualitatively different optimization landscapes, raising the question of what underlying task properties drive the difference.

An empirical bilinear form. We fit a parametric

model to the sub-ceiling cells ($V < 0.97$), with log fitness gap as the response and depth and breadth as predictors:

$$\log(1-V) = \beta_0 + a \log T + b \log N + c \log T \log N. \quad (2)$$

A budget-only model ($c=0$, $a=b$) reaches $R^2 \approx 0.74$ – 0.78 ; the bilinear form reaches $R^2 \in [0.75, 0.92]$ across all three tasks (Table 1). Allocation, with budget, carries the signal. The coefficient c characterizes the regime (interior at large negative $|c|$, corner near $|c| \approx 0$; full boundary analysis in Appendix F.3) in a way prior inference-time scaling work reports descriptively but does not pin down (Snell et al., 2024; Inoue et al., 2025); higher-order terms ($\log^2 T$, $\log^2 N$) do not materially improve the fit (Appendix F).

Among the four coefficients, c alone controls geometry: small $|c|$ leaves the budget slice near-separable with the optimum at the all-depth corner, while large negative $|c|$ bends it inward to a balanced interior optimum, with plateau half-width $\propto 1/\sqrt{|c|}$ (Appendix F.2). MMD sits in the latter limit on both capable models; CP and HT sit in the former (Table 1, with the near-zero rows discussed in Appendix F.3). The case studies (Appendix D) are consistent with a mechanism we call *asymmetric proposal mass*: each task admits one high-fitness algorithmic family, but the LLM’s base rate on it appears differ across tasks, so where the good family is rare, breadth raises the probability that at least one parallel trajectory anchors on it

before depth can refine within it.

6 Modeling Evolving Trajectory through Multi-Armed Bandits

Evolve Trajectory Analysis. Section 5 characterized within-run depth-breadth allocation on capable model and task. However, the self-evolving process itself remains highly stochastic. Specifically, we run the experiments multiple times under the same allocation configuration (sequential: $T = 512, N = 1$) and analyze each *greedy* run’s performance by tracing its fitness score trajectory throughout the game in Figure 4. Evolving may dramatically fail from time to time by converging at a low score without further improvement even under the *same configuration*, producing a distribution (Appendix E) rather than a single value (Appendix D), a spread that within-run allocation cannot remove. A second allocation lever is therefore needed, one that operates between trajectories rather than within them.

We instantiate the cross-trajectory lever as a multi-armed bandit (MAB) over K parallel runs. Each arm corresponds to one trajectory initialized from the same seed program; each pull spends one LLM call extending that trajectory and reveals its new fitness. The policy’s decision after every call, i.e., which arm to pull next, routes budget away from stagnating runs and toward more promising ones.

6.1 Bandits Adaptation

MAB provides a framework for sequential decision-making in uncertain environments. In the standard setting, the player chooses an action to take from a finite action set $[K]$ at each round $c \in [C] := \{1, 2, \dots, C\}$ and observes the associated reward, which may immediately factor into the decision in the next round. Deploying Improving Bandits (Heidari et al., 2016) as the backbone, we propose our adaptive self-evolving algorithm, namely, Bandits-based Self-Evolving (BaSE), in Algorithm 2.

Intuitively, Algorithm 2 treats self-evolution as a *cross-trajectory allocation* problem. Under the same fixed LLM-call budget, a single-trajectory method spends all generations on one evolving path, whereas BaSE allocates the budget across K parallel trajectories and adaptively decides which trajectory should receive the next call. Each arm corresponds to one evolving trajectory initialized from the same seed program, and the bandit policy

Algorithm 2 Bandits-based Self-Evolving (BaSE)

Require: Task q , base LLM f , prompt generator h , budget (number of LLM calls) C , number of runs K

- 1: Initialize $c_i \leftarrow 1$ for all $i \in [K]$
- 2: **for all** $i \in [K]$ **in parallel do**
- 3: prompt $\leftarrow h(q)$
- 4: response $_i^{(c_i)} \leftarrow f(\text{prompt})$
- 5: score $_i \leftarrow \text{Eval}(q, \text{response}_i^{(c_i)})$
- 6: **end for**
- 7: **for** $c = K + 1, \dots, C$ **do**
- 8: $i \leftarrow \text{MAB}(1, \dots, K)$
- 9: prompt $\leftarrow h\left(q, \left(\text{response}_i^{(j)}, \text{score}_i^{(j)}\right)_{j \in [c_i]}\right)$
- 10: response $_i^{(c_i+1)} \leftarrow f(\text{prompt})$
- 11: score $_i^{(c_i+1)} \leftarrow \text{Eval}(q, \text{response}_i^{(c_i+1)})$
- 12: $c_i \leftarrow c_i + 1$
- 13: **end for**
- 14: $(i^*, j^*) \leftarrow \arg \max_{i \in [K], j \in [c_i]} \text{score}_i^{(j)}$
- 15: **return** response $_{i^*}^{(j^*)}$

only decides which trajectory should reveal its next point in an online manner. It does not alter the local refinement rule or change how a selected trajectory evolves. In this sense, BaSE improves search by reallocating computation across heterogeneous trajectories rather than by modifying the trajectory dynamics themselves.

6.2 Our Results

Fitness Score. As shown in Table 2, we report the average fitness score across three tasks, model families, and self-evolving strategies at $C = 512$ generations. BaSE achieves the best or near-best fitness across different model families and scales. For example, Thompson reaches 0.8736 on Qwen3-8B HT, clearly above greedy (0.6780) and ShinkaEvolvo (0.7379); on Llama HT, it obtains 0.4387, outperforming all baselines by a large margin; and on Qwen3-14B CP, it attains the highest average fitness score of 1.0003.

The improvement reflects the value of allocating the fixed budget across multiple evolving trajectories, rather than modifying the refinement dynamics within a trajectory, while keeping the total LLM-call budget fixed. Indeed, under the same fixed computation (generation) budget, trajectory diversification itself helps avoid committing the full budget to a low-potential run but adaptively allocates budget to more promising trajectories.

Although BaSE attains the strongest mean across all reported model-task pairs, we note that the magnitude of the improvement varies with task difficulty and available headroom. On saturated

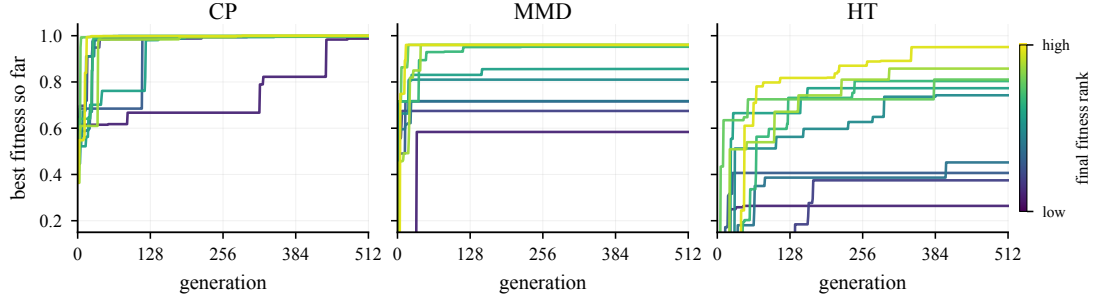


Figure 4: Per-run greedy fitness trajectories at $T=512$, $N=1$ on Qwen3-8B. Greedy reliably reaches high fitness in CP, while several seeds in MMD and HT stagnate at suboptimal values.

Table 2: Fitness scores (mean \pm SE) across models, tasks, and evolution strategies at 512 LLM calls ($C=512$). The maximum fitness score in each (model, task) is **bolded**.

Model	Task	Baselines				BaSE		
		Greedy	OpenEvolve	CodeEvolve	ShinkaEvolve	UCB	EXP3.P	Thompson
Qwen3-8B	CP	0.9985 \pm .0005	0.8279 \pm .0145	0.7692 \pm .0202	0.9986 \pm .0003	0.9965 \pm .0102	0.9993 \pm .0059	1.0003 \pm .0174
	MMD	0.9597 \pm .0039	0.9561 \pm .0143	0.8414 \pm .0689	0.9099 \pm .0240	0.9603 \pm .0053	0.9658 \pm .0102	0.9603 \pm .0035
	HT	0.6780 \pm .0718	0.6061 \pm .0768	0.5168 \pm .0627	0.7379 \pm .0373	0.8530 \pm .0963	0.8653 \pm .1068	0.8736 \pm .1737
Llama	CP	0.8432 \pm .0496	0.7033 \pm .0657	0.4568 \pm .0330	0.8305 \pm .0362	0.9451 \pm .0633	0.9484 \pm .0716	0.9533 \pm .0706
	MMD	0.8424 \pm .0215	0.6378 \pm .1024	0.2315 \pm .0847	0.7253 \pm .0453	0.9512 \pm .1020	0.8516 \pm .1072	0.8634 \pm .0955
	HT	0.2538 \pm .0762	0.0000 \pm .0000	0.0000 \pm .0000	0.1512 \pm .0437	0.2561 \pm .1196	0.2729 \pm .1851	0.4387 \pm .2134
Qwen3-14B	CP	0.9802 \pm .0060	0.8577 \pm .0228	0.8768 \pm .0134	0.9981 \pm .0003	0.9972 \pm .0074	0.9967 \pm .0114	1.0003 \pm .0143
	MMD	0.9816 \pm .0059	0.9949 \pm .0012	0.9934 \pm .0021	0.9924 \pm .0037	0.9969 \pm .0356	0.9922 \pm .0283	0.9983 \pm .0163

tasks such as CP, several baselines already approach the score ceiling; for example, Qwen3-8B greedy and ShinkaEvolve achieve 0.9985 and 0.9986, while BaSE-Thompson reaches 1.0003 with CI [0.9980, 1.0004]. Hence, the CP gains are necessarily small. By contrast, BaSE shows clearer benefits on harder settings such as HT, where Qwen3-8B BaSE-Thompson reaches 0.8736 compared with the best non-BaSE score of 0.7379, and Llama BaSE-Thompson reaches 0.4387 while all non-BaSE methods remain below 0.2538.

Cross-Trajectory Allocation with Parent Sampling Protocols. BaSE is orthogonal to parent-sampling strategies: BaSE decides which trajectory receives the next LLM call, while parent sampling decides which historical response is used to refine the selected trajectory. Thus, [Line 9 in Algorithm 2](#) can replace the vanilla prompt generator with existing parent-sampling methods. In [Appendix G.1](#), we evaluate this combination by pairing BaSE with different parent-sampling baselines and comparing against greedy variants under different breadth-depth allocations. As shown in [Table 8](#), these strategies can be naturally integrated into BaSE, often improving their best fitness scores, especially in unstable settings with high trajectory variance.

Sample-Efficient Threshold Reaching. Beyond final fitness, we evaluate how efficiently each method reaches a target fitness threshold τ under a fixed budget. Following the time-to-threshold metric of [Taylor et al. \(2007\)](#), we report the earliest generation G and corresponding cumulative FLOPs at which 90% of bootstrap samples reach τ . As shown in [Table 3](#), BaSE reaches most thresholds with fewer generations and FLOPs, especially on MMD and HT. For example, on MMD, UCB reaches $\tau = 0.95$ at 92 generations, while greedy requires 485; on HT, UCB reaches $\tau = 0.70$ within 60 generations, whereas greedy, OpenEvolve, and CodeEvolve never reach it. Compared with random allocation, Thompson reaches the same thresholds with $\sim 40\%$ fewer generations on average across the seven reached cells. Full results across three models are deferred to [Appendix G.2](#).

Ablation on Arm-Pool Size. We ablate the number of parallel runs K (number of arms) used by BaSE and defer the full results to [Appendix G.3 \(Table 10\)](#). The results show that moderate arm pools usually provide the best trade-off between trajectory diversity and per-run refinement depth. In particular, $K \in \{5, 10, 20\}$ often achieves the strongest performance, while very small pools can

Table 3: Minimum generation (Gen.) and cumulative FLOPs ($\times 10^{15}$) required for $\geq 90\%$ samples to reach thresholds ($\geq \tau$) with Qwen3-8B as the base LLM. Unreached thresholds are denoted as “—”. The minimum generation and FLOPs for each threshold are **bolded**.

Task	τ	Baselines								BaSE							
		Greedy		OpenEvolve		CodeEvolve		ShinkaEvolve		Rand		UCB		EXP3.P		Thompson	
		Gen.	FLOPs	Gen.	FLOPs	Gen.	FLOPs	Gen.	FLOPs	Gen.	FLOPs	Gen.	FLOPs	Gen.	FLOPs	Gen.	FLOPs
CP	0.95	152	182.12	—	—	—	—	45	57.90	56	66.58	16	18.19	139	173.57	16	18.19
	0.99	359	411.93	—	—	—	—	73	90.15	138	170.88	85	100.79	207	256.12	85	101.22
	0.999	—	—	—	—	—	—	—	—	—	—	—	—	—	—	327	395.47
MMD	0.80	212	318.46	119	181.48	—	—	71	112.00	26	32.34	8	12.41	40	52.72	8	12.41
	0.90	296	436.55	—	—	—	—	—	—	119	179.07	92	117.63	95	142.59	105	144.75
	0.95	485	656.81	—	—	—	—	—	—	132	199.95	92	117.63	114	172.74	106	146.75
HT	0.50	—	—	—	—	—	—	201	189.28	92	99.90	60	66.90	102	108.67	74	79.45
	0.70	—	—	—	—	—	—	—	—	367	381.23	125	130.55	209	213.22	101	104.53

lack sufficient exploration and overly large pools such as $K = 50$ may dilute the refinement budget across too many shallow trajectories.

7 Discussion

Allocation wins, not prompt engineering. The CP results in Table 2 appear to make ShinkaEvolve a rather strong baseline (0.9986 on Qwen3-8B), while inspection of the prompts in Appendix H shows this advantage could be prompt-induced: ShinkaEvolve’s CP system prompt explicitly suggests `scipy.optimize`. While our method use exactly the same prompt as OpenEvolve, steering away from quick-win hints. Our greedy baseline reaches 0.9985 on the same task, which is a +0.17 gap over OpenEvolve. As Appendix D documents, this gap is the LLM eventually discovering `scipy` despite the prompt discouraging it, not on top of a privileged prompt.

Model capability and prompt set the ceiling that allocation can reach. Allocation amplifies an existing signal but cannot create one. On Llama HT (Table 2), OpenEvolve and CodeEvolve collapse to 0.0 (no run produces a valid configuration in 512 calls) and even Thompson only recovers to 0.4387, an order of magnitude below Qwen3-8B on the same task. Appendix C shows the same pattern across the full sweep: when a model fails to cross the capability threshold on relatively difficult task, depth gains are statistically indistinguishable from selection noise. The prompt sets a separate ceiling: ShinkaEvolve’s HT prompt (Appendix H) contains a “CRITICAL — degeneracy warning” about collinear-triplet failures that no other baseline carries, and this directly addresses the failure mode diagnosed in Appendix D (HT run 5). Capability and prompt thus jointly determine the achiev-

able ceiling; allocation governs how efficiently a method approaches it.

BaSE is complementary to within-run mechanisms. BaSE operates at trajectory granularity, while the parent-sampling protocols in *Evolve systems operate within a single run; the two compose. The improvement of BaSE over a single-trajectory baseline admits a clean two-step decomposition: *Greedy/Island* \rightarrow *Random* isolates the pool effect (drawing K independent trajectories and returning the best), and *Random* \rightarrow BaSE isolates the allocation effect (adaptively routing compute toward promising trajectories). The pool effect is licensed by the per-run heterogeneity documented in Figure 4 and Appendix D. The allocation effect is then isolated by the Random vs. BaSE gap in Table 3. Both effects survive when BaSE replaces the prompt generator of OpenEvolve, CodeEvolve, or ShinkaEvolve (Table 8 in Appendix G.1), with the largest gains where the underlying protocol leaves trajectory variance unexploited and the smallest where it has already saturated the task.

8 Conclusion

In conclusion, we presented the first fixed-budget characterization of depth–breadth allocation in LLM-guided evolutionary search, revealing structured, task-dependent fitness surfaces and an empirical bilinear regularity. We then showed that fixed allocations still leave substantial cross-trajectory heterogeneity. Motivated by this observation, we introduced BaSE, a bandit-based allocator that improves expected fitness and threshold-reaching efficiency over strong *Evolve baselines without changing the base model, evaluator, or prompt design. This highlights compute allocation as a key lever for reliable finite-budget search.

References

- Rishabh Agarwal, Max Schwarzer, Pablo Samuel Castro, Aaron Courville, and Marc G. Bellemare. 2022. [Deep reinforcement learning at the edge of the statistical precipice](#). *Preprint*, arXiv:2108.13264.
- Shipra Agrawal and Navin Goyal. 2012. Analysis of thompson sampling for the multi-armed bandit problem. In *Conference on learning theory*, pages 39–1. JMLR Workshop and Conference Proceedings.
- Henrique Assumpção, Diego Ferreira, Leandro Campos, and Fabricio Murai. 2025. [CodeEvolve: an open source evolutionary coding agent for algorithmic discovery and optimization](#). *arXiv preprint arXiv:2510.14150*.
- Jean-Yves Audibert and Sébastien Bubeck. 2010. Best arm identification in multi-armed bandits. In *COLT-23th Conference on learning theory-2010*, pages 13–p.
- Peter Auer, Nicolò Cesa-Bianchi, and Paul Fischer. 2002a. Finite-time analysis of the multiarmed bandit problem. *Machine Learning*, 47(2):235–256.
- Peter Auer, Nicolò Cesa-Bianchi, Yoav Freund, and Robert E Schapire. 2002b. The nonstochastic multi-armed bandit problem. *SIAM journal on computing*, 32(1):48–77.
- Golnaz Badkobeh, Per Kristian Lehre, and Dirk Sudholt. 2014. [Unbiased black-box complexity of parallel search](#). In *Parallel Problem Solving from Nature – PPSN XIII*, pages 892–901. Springer International Publishing.
- Martin Briesch, Dominik Sobania, and Franz Rothlauf. 2023. [On the trade-off between population size and number of generations in GP for program synthesis](#). In *Proceedings of the Companion Conference on Genetic and Evolutionary Computation (GECCO Companion)*, pages 535–538. ACM.
- Bradley Brown, Jordan Juravsky, Ryan Ehrlich, Ronald Clark, Quoc V. Le, Christopher Ré, and Azalia Mirhoseini. 2024. [Large language monkeys: Scaling inference compute with repeated sampling](#). *arXiv preprint arXiv:2407.21787*.
- Mert Cemri, Shubham Agrawal, Akshat Gupta, Shu Liu, Audrey Cheng, Qiuyang Mang, Ashwin Naren, Lutfi Eren Erdogan, Koushik Sen, Matei Zaharia, Alex Dimakis, and Ion Stoica. 2026. [AdaEvolve: Adaptive LLM driven zeroth-order optimization](#). *arXiv preprint arXiv:2602.20133*.
- Angelica Chen, David M. Dohan, and David R. So. 2023. [EvoPrompting: Language models for code-level neural architecture search](#). *arXiv preprint arXiv:2302.14838*.
- Yanxi Chen, Xuchen Pan, Yaliang Li, Bolin Ding, and Jingren Zhou. 2024. [Provable scaling laws for the test-time compute of large language models](#). *arXiv preprint arXiv:2411.19477*. NeurIPS 2025.
- Benjamin Doerr and Marvin Künnemann. 2015. [Optimizing linear functions with the \$\(1 + \lambda\)\$ evolutionary algorithm—different asymptotic runtimes for different instances](#). *Theoretical Computer Science*, 561:3–23.
- Christian Gießen and Carsten Witt. 2017. [The interplay of population size and mutation probability in the \$\(1 + \lambda\)\$ EA on OneMax](#). *Algorithmica*, 78(2):587–609.
- Hoda Heidari, Michael Kearns, and Aaron Roth. 2016. Tight policy regret bounds for improving and decaying bandits. In *Proceedings of the Twenty-Fifth International Joint Conference on Artificial Intelligence, IJCAI’16*, page 1562–1570. AAAI Press.
- Jordan Hoffmann, Sebastian Borgeaud, Arthur Mensch, Elena Buchatskaya, Trevor Cai, Eliza Rutherford, Diego de Las Casas, Lisa Anne Hendricks, Johannes Welbl, Aidan Clark, Tom Hennigan, Eric Noland, Katie Millican, George van den Driessche, Bogdan Damoc, Aurelia Guy, Simon Osindero, Karen Simonyan, Erich Elsen, and 3 others. 2022. [Training compute-optimal large language models](#). *Preprint*, arXiv:2203.15556.
- Yuichi Inoue, Kou Misaki, Yuki Imajuku, So Kuroki, Taishi Nakamura, and Takuya Akiba. 2025. [Wider or deeper? scaling llm inference-time compute with adaptive branching tree search](#). *Preprint*, arXiv:2503.04412.
- Thomas Jansen, Kenneth A. De Jong, and Ingo Wegener. 2005. On the choice of the offspring population size in evolutionary algorithms. *Evolutionary Computation*, 13(4):413–440.
- Thomas Jansen and Christine Zarges. 2012. [Fixed budget computations: a different perspective on run time analysis](#). In *Proceedings of the 14th Annual Conference on Genetic and Evolutionary Computation (GECCO)*, pages 1325–1332.
- Thomas Jansen and Christine Zarges. 2014. Performance analysis of randomised search heuristics operating with a fixed budget. *Theoretical Computer Science*, 545:39–58.
- Zohar Karnin, Tomer Koren, and Oren Somekh. 2013. [Almost optimal exploration in multi-armed bandits](#). In *Proceedings of the 30th International Conference on Machine Learning*, volume 28 of *Proceedings of Machine Learning Research*, pages 1238–1246, Atlanta, Georgia, USA. PMLR.
- Robert Lange, Tom Schaul, Yutian Chen, Tom Zahavy, Valentin Dalibard, Chris Lu, Satinder Singh, and Sebastian Flennerhag. 2023. Discovering evolution strategies via meta-black-box optimization. In *Proceedings of the companion conference on genetic and evolutionary computation*, pages 29–30.
- Robert Tjarko Lange, Yuki Imajuku, and Edoardo Cetin. 2025. [ShinkaEvolve: Towards open-ended and sample-efficient program evolution](#). *arXiv preprint arXiv:2509.19349*.
- Tor Lattimore and Csaba Szepesvári. 2020. *Bandit Algorithms*. Cambridge University Press.
- Kuang-Huei Lee, Ian Fischer, Yueh-Hua Wu, Dave Marwood, Shumeet Baluja, Dale Schuurmans, and Xinyun Chen. 2025. [Evolving deeper llm thinking](#). *Preprint*, arXiv:2501.09891.

- Joel Lehman, Jonathan Gordon, Shawn Jain, Kamal Ndousse, Cathy Yeh, and Kenneth O. Stanley. 2022. [Evolution through large models](#). *arXiv preprint arXiv:2206.08896*.
- Lisha Li, Kevin Jamieson, Giulia DeSalvo, Afshin Ros-tamizadeh, and Ameet Talwalkar. 2018. Hyperband: A novel bandit-based approach to hyperparameter optimization. *Journal of Machine Learning Research*, 18(185):1–52.
- Elliot Meyerson, Mark J Nelson, Herbie Bradley, Adam Gaier, Arash Moradi, Amy K Hoover, and Joel Lehman. 2024. Language model crossover: Variation through few-shot prompting. *ACM Transactions on Evolutionary Learning*, 4(4):1–40.
- Sora Miyamoto, Daisuke Oba, and Naoaki Okazaki. 2026. [Aligning tree-search policies with fixed token budgets in test-time scaling of LLMs](#). *arXiv preprint arXiv:2602.09574*.
- Jean-Baptiste Mouret and Jeff Clune. 2015. Illuminating search spaces by mapping elites. *arXiv preprint arXiv:1504.04909*.
- Ryohei Nakano, Yuval Davidor, and Takeshi Yamada. 1994. [Optimal population size under constant computation cost](#). In *Parallel Problem Solving from Nature – PPSN III*, pages 130–138. Springer Berlin Heidelberg.
- Alexander Novikov, Ngân Vũ, Marvin Eisenberger, Emilien Dupont, Po-Sen Huang, Adam Zsolt Wagner, Sergey Shirobokov, Borislav Kozlovskii, Francisco J. R. Ruiz, Abbas Mehrabian, M. Pawan Kumar, Abigail See, Swarat Chaudhuri, George Holland, Alex Davies, Sebastian Nowozin, Pushmeet Kohli, and Matej Balog. 2025. [AlphaEvolve: A coding agent for scientific and algorithmic discovery](#). *arXiv preprint arXiv:2506.13131*.
- Bernardino Romera-Paredes, Mohammadamin Barekatin, Alexander Novikov, Matej Balog, M. Pawan Kumar, Emilien Dupont, Francisco J. R. Ruiz, Jordan S. Ellenberg, Pengming Wang, Omar Fawzi, Pushmeet Kohli, and Alhussein Fawzi. 2024. [Mathematical discoveries from program search with large language models](#). *Nature*, 625(7995):468–475.
- Aman Sharma and Paras Chopra. 2025. [The sequential edge: Inverse-entropy voting beats parallel self-consistency at matched compute](#). *arXiv preprint arXiv:2511.02309*.
- Chengshuai Shi, Kun Yang, Zihan Chen, Jundong Li, Jing Yang, and Cong Shen. 2024. Efficient prompt optimization through the lens of best arm identification. In *Advances in Neural Information Processing Systems (NeurIPS)*. ArXiv:2402.09723.
- Charlie Snell, Jaehoon Lee, Kelvin Xu, and Aviral Kumar. 2024. [Scaling LLM test-time compute optimally can be more effective than scaling model parameters](#). *arXiv preprint arXiv:2408.03314*.
- Reiko Tanese. 1989. *Distributed Genetic Algorithms for Function Optimization*. Ph.D. thesis, University of Michigan, Ann Arbor, MI. ProQuest Dissertations & Theses, 9001722.
- Hao Tang, Keya Hu, Jin Peng Zhou, Sicheng Zhong, Wei-Long Zheng, Xujie Si, and Kevin Ellis. 2024. [Code repair with LLMs gives an exploration-exploitation tradeoff](#). In *Advances in Neural Information Processing Systems (NeurIPS)*.
- Matthew E. Taylor, Peter Stone, and Yaxin Liu. 2007. [Transfer learning via inter-task mappings for temporal difference learning](#). *Journal of Machine Learning Research*, 8(73):2125–2167.
- William R Thompson. 1933. On the likelihood that one unknown probability exceeds another in view of the evidence of two samples. *Biometrika*, 25(3/4):285–294.
- Yiping Wang, Shao-Rong Su, Zhiyuan Zeng, Eva Xu, Liliang Ren, Xinyu Yang, Zeyi Huang, Xuehai He, Luyao Ma, Baolin Peng, Hao Cheng, Pengcheng He, Weizhu Chen, Shuohang Wang, Simon Shaolei Du, and Weizhong Shen. 2025. [ThetaEvolve: Test-time learning on open problems](#). *arXiv preprint arXiv:2511.23473*.
- Hao Wen, Yifan Su, Feifei Zhang, Yunxin Liu, Yunhao Liu, Ya-Qin Zhang, and Yuanchun Li. 2025. [Para-Thinker: Native parallel thinking as a new paradigm to scale LLM test-time compute](#). *arXiv preprint arXiv:2509.04475*.
- Yangzhen Wu, Zhiqing Sun, Shanda Li, Sean Welleck, and Yiming Yang. 2024. [Inference scaling laws: An empirical analysis of compute-optimal inference for problem-solving with language models](#). *arXiv preprint arXiv:2408.00724*.
- Chengrun Yang, Xuezhi Wang, Yifeng Lu, Hanxiao Liu, Quoc V. Le, Denny Zhou, and Xinyun Chen. 2023. [Large language models as optimizers](#). *arXiv preprint arXiv:2309.03409*.
- Yanzhi Zhang, Yitong Duan, Zhaoxi Zhang, Jiyan He, and Shuxin Zheng. 2025. [Population-Evolve: a parallel sampling and evolutionary method for LLM math reasoning](#). *arXiv preprint arXiv:2512.19081*.

Appendix Contents

A Effective FLOPs	11
B Task Details	11
C The Capability Gate of the Collapse	12
D Case Studies: Why Runs Stagnate	12
D.1 Circle Packing: scipy acquisition is the gating event	13
D.2 MinMaxDist: the analytic attractor wins; scipy <i>poisons</i> the run . . .	13
D.3 Heilbronn Triangle: the same mechanism, with stricter feasibility	15
E Distribution	15
F Depth–Breadth Regularity	16
F.1 Robustness to Richer Specifications	16
F.2 Plateau Width and Online Search .	17
F.3 Boundary of the Regime	18
G Deferred BaSE Experiments	18
G.1 Pairwise Fitness Comparisons . .	18
G.2 Full Threshold Comparison	19
G.3 Ablation on Bandit Arm-Pool Size	20
H Prompts	20
H.1 OpenEvolve (also used by Greedy and BaSE)	21
H.2 CodeEvolve	23
H.3 ShinkaEvolve	25
I Use of AI Assistants	26
J Artifact Licenses	27
K Ethics Statement	27
L Potential Risks	27

A Effective FLOPs

The protocols differ in cache behavior as a structural consequence of their prompt construction, where greedy reuses a single parent prefix across batched siblings in a generation, while island rewrites the parent + inspirations per call.

Formula. We charge each completed LLM call

$$\text{FLOPs}_{\text{call}} = 2 P_{\text{active}} (p_{\text{uncached}} + p_{\text{out}}),$$

where P_{active} is the active parameter count, $p_{\text{uncached}} = p_{\text{prompt}} - p_{\text{cached}}$, and p_{out} is the completion token count. Per-run FLOPs sums over all attempts, including retries. Token counts and cache statistics are read directly from vLLM’s per-request usage records. The factor $2 P_{\text{active}}$ per token is the forward-pass cost in the $C \approx 6ND$ in the spirit of Chinchilla (Hoffmann et al., 2022), using only the forward $2N$ component as no backward pass occurs in LLM-guided evolution. As in Chinchilla, this convention omits sub-leading terms (attention score computation, softmax, layer norms, embeddings, sampling); Chinchilla’s reports agreement with detailed accounting to within 10% over two orders of magnitude.

Active parameters. All models in our sweep (Qwen3 1.7B/4B/8B/14B and Llama-3.1-8B) are dense, so P_{active} equals the total parameter count. The notation is retained for compatibility with MoE models.

Prefix-cached tokens. Cached prompt tokens are subtracted because vLLM’s PagedAttention reuses their KV states without recomputing the corresponding forward pass. Cache hit rates in our sweeps range from 94% to 98%; omitting this subtraction over-reports FLOPs by 6–9%. The residual attention computation over cached tokens is sub-leading and is omitted, consistent with the convention above.

Non-embedding variant. Some scaling-law conventions use non-embedding parameter counts in place of P_{active} . Substituting would multiply every reported FLOPs value by a fixed per-model factor $P_{\text{non-embed}}/P_{\text{active}}$, preserving all cross-model ratios and orderings used in our analysis.

B Task Details

For all three tasks, raw objectives are normalized by the best published construction so that $\text{FITNESS}=1.0$ matches the state of the art:

Circle Packing (CP, $n=26$). Pack 26 non-overlapping circles into the unit square to maximize the sum of their radii. Fitness is normalized to the AlphaEvolve reference of 2.635 for $n = 26$, so normalizer: $\text{FITNESS} = \text{SUM}_{\text{radii}}/2.635$.

MinMaxDist (MMD, $n=16, d=2$). Place 16 points in the plane to maximize the ratio of minimum to maximum pairwise distance, d_{\min}/d_{\max} . Fitness is the squared ratio normalized to the benchmark of $1/\sqrt{12.889266112} \approx 0.2786$, normalizer: $\text{FITNESS} = (d_{\min}/d_{\max})^2 \cdot 12.889266112$; The configuration space contains a sharp deterministic attractor at fitness ≈ 0.9603 corresponding to a 5+11 construction.

Heilbronn Triangle (HT, $n=11$). Place 11 points on or inside the equilateral triangle with vertices $(0, 0)$, $(1, 0)$, and $(0.5, \sqrt{3}/2)$. The evaluator enumerates all $\binom{11}{3}$ triplets and computes the smallest triangle area, normalized by the area of the containing equilateral triangle. The final score divides this normalized minimum area by the reference $r_{\text{AE}} = 0.036529889880030156$.

Note that subsequent *Evolve runs have marginally surpassed the 2.635 AlphaEvolve CP reference, so FITNESS values slightly above 1.0 reflect this margin rather than a novel construction; we retain 2.635 as the normalizer for harness consistency with prior work.

C The Capability Gate of the Collapse

The fitness–FLOPs envelope of Section 5.1 collapses across model size only partially: capable models lie on one curve, weaker ones fall below it. To characterise the boundary we compute, per model×task cell, the best-of- N fitness $V_{T=1}$, the best mean fitness over all tested depths V_{\max} , the depth gain $\text{penBoN} = V_{\max} - V_{T=1}$, and a permutation p -value for that gain (Table 4).

Under the null that depth has no effect, we shuffle per-seed fitness across T , recompute penBoN on each shuffle, and let p be the fraction of 20,000 shuffles meeting or exceeding the observed value. A bootstrap CI is uninformative because V_{\max} already takes a max over ~ 10 depth cells, forcing $\text{penBoN} \geq 0$ on every resample; the permutation null re-maxes too and so absorbs that selection inflation.

The depth signal turns on with scale within Qwen3. At 1.7B penBoN is small and not significant on

Table 4: Capability gate per model×task cell. $V_{T=1}$ is the best-of- N fitness, V_{\max} the best over all depths, $\text{penBoN} = V_{\max} - V_{T=1}$, and p the depth permutation test. 1.7B/4B evaluated at $C=128$, all others at $C=512$.

Model	Task	$V_{T=1}$	V_{\max}	penBoN	p
1.7B	CP	0.582	0.615	+0.033	0.48
4B	CP	0.738	0.790	+0.052	0.30
8B	CP	0.989	0.999	+0.009	0.13
14B	CP	0.926	0.980	+0.054	0.07
Llama	CP	0.843	0.843	+0.000	1.00
1.7B	MMD	0.716	0.748	+0.031	0.16
4B	MMD	0.694	0.906	+0.213	0.002
8B	MMD	0.944	0.960	+0.016	0.64
14B	MMD	0.867	0.981	+0.115	$<10^{-3}$
Llama	MMD	0.673	0.843	+0.170	0.23
8B	HT	0.339	0.672	+0.333	0.002
Llama	HT	0.047	0.253	+0.206	0.013

either task ($p \geq 0.16$). At 4B it appears on MMD (+0.213, $p = 0.002$) but not on CP ($p = 0.30$). On CP and MMD, 8B and 14B reach $V_{\max} \geq 0.96$ on every tested cell, near the task ceiling, and depth gains compress to small residuals, while the exception is 14B/MMD, +0.115 at $p < 10^{-3}$. On the unsaturated HT task, 8B/HT instead shows the largest clean depth gain in the table: V rises from 0.339 to 0.672 (+0.333, $p = 0.002$). The depth signal therefore turns on whenever a capable model has room above best-of- N . The threshold is per (model, task), not per model: 4B sits on either side depending on the task.

Most striking is Llama-3.1-8B. On CP best-of- N already reaches 0.843 and depth does not improve it ($\text{penBoN} = 0, p = 1.00$). On MMD the nominal +0.170 depth gain is consistent with max-selection noise ($p = 0.23$). On HT depth does compound (V rises from 0.047 to 0.253 at $p = 0.013$), but the absolute level stays at 0.25, far below the 0.67 that Qwen3-8B reaches on the same task. Despite its 8B parameters, Llama-3.1-8B never achieves both a significant depth gain and a non-trivial absolute level on any tested task. Crossing the threshold is thus not a matter of parameter count.

D Case Studies: Why Runs Stagnate

The main text (Figure 4) shows that ten greedy runs of an identical configuration produce very different final fitness: some climb smoothly, others stop improving early and sit at a low score for the rest of the $C=512$ budget. This appendix opens up that variability and asks, at the level of the actual Python code the LLM produced, *why* certain runs

get stuck.

Each run is a chain of accepted programs. At every generation, greedy keeps the single best-scoring program seen so far and asks the LLM to mutate it. A child is accepted only if it strictly beats this running best. So a run gets “stuck” when, for many generations in a row, the LLM proposes mutations that the evaluator either rejects (returns a worse score) or cannot score at all (invalid output). To understand a stuck run we therefore have to look at two things: (i) what program the run is anchored on, and (ii) why no proposed mutation beats it.

Figure 5 shows one healthy and one stuck run per task, using the actual point/circle configurations the anchored program outputs. The rest of this appendix walks through each task in turn.

D.1 Circle Packing: *scipy* acquisition is the gating event

The task in one sentence. Pack 26 non-overlapping circles into the unit square so that the sum of their radii is as large as possible; the AlphaEvolve reference is $\sum_i r_i = 2.635$, according fitness=1.0 base on this sum of radii matches the state of the art.

Two regimes the LLM oscillates between. On CP the LLM writes programs that fall into two clearly different families:

- (a) *Hand-coded ring constructors*: the program lays 26 circles down in geometric rows (e.g. 6+5+6+5+4 hexagonal rows) and assigns each circle the same fixed radius based on the row spacing. No optimization is performed. The best score this family can produce in our runs is ~ 0.89 , because uniform radii waste space in the corners and at the row endings.
- (b) *scipy.optimize.minimize-based programs*: the same row layout is used as an initial guess, but the program then calls SLSQP or COBYLA with non-overlap and box-containment constraints, letting both centers and radii float. These programs reach ~ 1.0 .

Acquiring *scipy* is therefore the gating event for high fitness on CP: every run that finishes above 0.99 is anchored on a *scipy* program; the one run that does not is the one where the LLM took longest to write a *scipy* call.

Healthy example — run 10. At generation 13, the LLM proposes the first child that imports *scipy* and wraps the ring layout in a constrained SLSQP call. The accepted score jumps from 0.5584 to 0.8396 in a single generation, a +0.28 improvement that no later generation matches. Within another three *scipy*-family accepts the run is at 0.9981 (gen 24); few more refinements over the next generations push it to $\sum_i r_i = 2.636$ (Figure 5).

Stuck example — run 6. The LLM proposes hand-coded ring constructors for the first 437 generations of this run. Within that family, the anchored program slowly improves through 5 accepts from 0.36 (initial) to 0.67 (gen 88), then sits at 0.67 for 233 generations, then jumps to 0.79 (gen 321) and 0.82 (gen 327) on two more ring-rewrites with non-hex vertical spacing, and freezes at 0.82 for another 110 generations. The displayed gen-437 best ($\sum_i r_i = 2.167$, panel “CP run 6 gen 437” in Figure 5) is the entire visible cost of this stretch: hundreds of attempts to improve a constructor whose intrinsic ceiling is below 0.89. The first *scipy* child finally arrives at generation 438, producing a +0.16 jump in one step (from 0.822 to 0.983).

D.2 MinMaxDist: the analytic attractor wins; *scipy* poisons the run

The task in one sentence. Place 16 points in the plane to maximize $(d_{\min}/d_{\max})^2$ — the squared ratio of the closest pair to the farthest pair — normalized so that fitness=1.0 matches the AlphaEvolve reference.

An analytic attractor exists. For this problem, the 5+11 regular-polygon construction — 5 points uniformly on an inner circle of radius r , 11 points uniformly on an outer circle of radius $R = r(1 + 2 \sin(\pi/5))$ — reaches the mathematical optimum for this split at fitness 0.9603. It involves no optimizer at all: just `np.linspace` and `np.cos/sin` calls in roughly fifteen lines of code.

***scipy* is the bad family on MMD.** Counter-intuitively to the CP story, on MMD the LLM’s *scipy*-based programs are exactly the ones that get stuck. Across the ten runs:

- 3 Runs finish above the attractor (0.9603), all *scipy*-free: pure analytic 5+11 polygons.
- 6 Runs finish below the attractor (0.58–

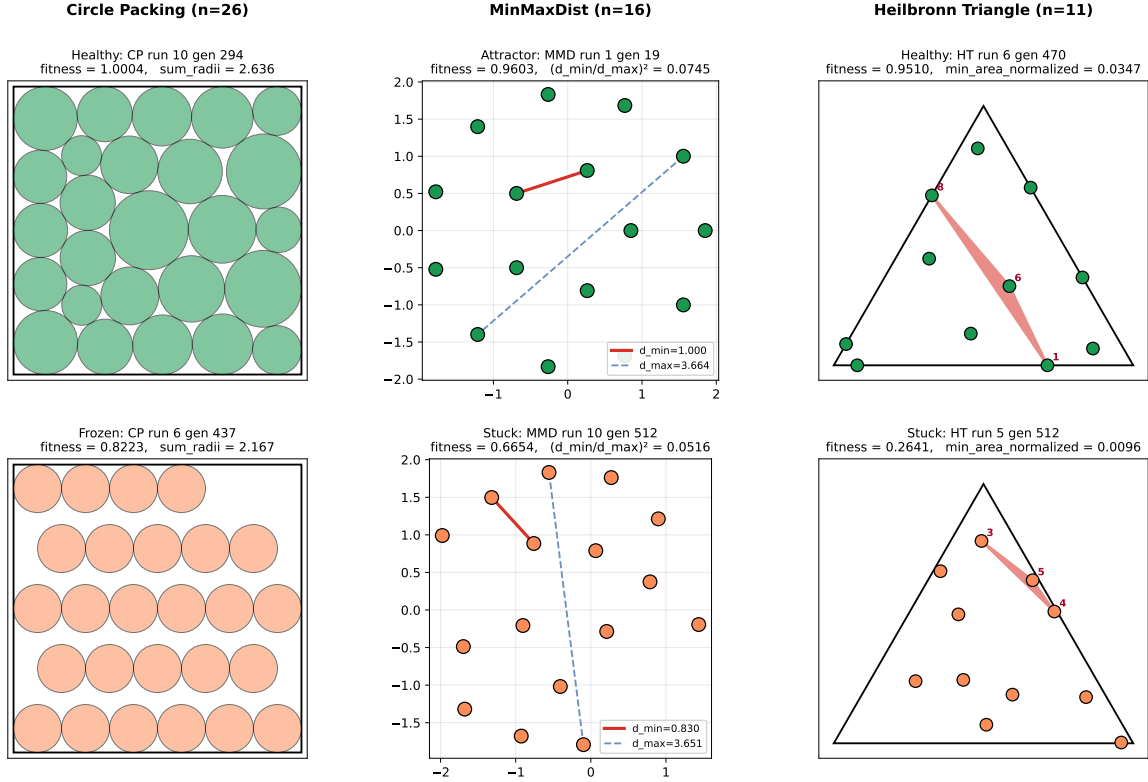


Figure 5: One healthy (top) and one stuck (bottom) greedy run per task at Greedy $T=512$, $N=1$ on Qwen3-8B. Each title gives the run number (out of 10), the generation at which the displayed program was the running best, the normalized fitness, and the task’s raw metric. **CP**: the unit square is filled with 26 non-overlapping circles; **MMD**: 16 points; the red bar is the closest pair (d_{\min}) and the blue dashed bar the farthest pair (d_{\max}); **HT**: 11 points inside the equilateral triangle; the red shaded triplet is the smallest of the $\binom{11}{3}=165$ triangles, which sets the score.

0.95). All six final programs call either `differential_evolution` or `minimize`, on an objective of the form $-(d_{\min}/d_{\max})^2$.

- Run 5 finishes at 0.86 without `scipy` but also without the polygon construction.

The reason the `scipy` programs fail is that the objective $-(d_{\min}/d_{\max})^2$ is highly non-convex; numerical optimizers from a generic initial guess (4×4 grid, 16-gon, etc.) converge to local optima where one pair of points is much closer than the rest, dragging d_{\min} down. The first such program greedy accepts becomes the run’s permanent anchor, because future proposed mutations have to beat its specific stochastic local optimum in a single re-evaluation.

Healthy Attractor example — run 1. The run climbs in 4 accepts from 0.02 (initial: 16 random Gaussian points) through intermediates (0.72, 0.86, 0.89) to 0.9603 at gen 19, where the LLM writes the closed-form polygon construction. The displayed gen-19 best (Figure 5) shows two clean concentric rings with all inner-to-outer distances

equal; the closest pair sits between adjacent outer points and the farthest pair spans a diameter.

Stuck example — run 10. The run accepts five different `scipy`-based programs (gens 2, 3, 5, 7, 8), cycling through `scipy.minimize` from a 16-gon, then concentric squares, then differential evolution from concentric circles, finally locking onto a differential evolution call from a 4×4 grid with strategy `rand1bin` at gen 8. By gen 8 the run is anchored at 0.6746. For the remaining 504 generations greedy accepts nothing. The displayed gen-512 best (Figure 5) shows the consequence: 14 of the 16 points are reasonably spread, but the DE local optimum happens to leave one pair noticeably closer than the rest — the red bar in the figure — and that single tight pair fixes d_{\min} at roughly 20% of d_{\max} .

On CP, `scipy`-based accepted programs score on average +0.35 higher than non-`scipy` ones (0.99 vs. 0.64); on MMD the sign flips, where `scipy` programs average -0.14 lower (0.59 vs. 0.73). Both tasks have a clear “correct” algorithmic family:

scipy for CP, analytic polygon for MMD. And both have a wrong family that imposes a hard ceiling. Whether greedy escapes depends entirely on which family it locks into first.

D.3 Heilbronn Triangle: the same mechanism, with stricter feasibility

The task in one sentence. Place 11 points on or inside the equilateral triangle with vertices $(0, 0)$, $(1, 0)$, $(0.5, \sqrt{3}/2)$ to maximize the area of the smallest triangle formed by any three of them.

HT differs from CP and MMD in two ways. First, the initial program returns 11 zeros and scores 0.0, so every run begins with a long stretch of invalid output — the LLM has to write *something* that puts 11 points inside the triangle before any fitness signal can be received. Second, there is no analytic attractor: every accepted improvement past the initial valid configuration is a numerical refinement, and the score is set by a single bottleneck triplet whose area must be enlarged without destroying the area of any of the other 164 triplets.

Healthy example — run 6. After 42 generations of invalid output, the run accepts its first valid configuration (score 0.2445) and then climbs through 13 further small accepts to 0.9510 at generation 470. The anchor program at gen 470 uses `scipy.optimize.minimize` with the SLSQP method, called from 100 randomly perturbed initial guesses, with *hard inequality constraints* for the three triangle edges (one constraint per point per edge) and a log-sum-exp soft-min ($\frac{1}{k} \log \sum_i e^{-ka_i}$, $k=1000$) over the 165 triplet areas as the objective. The three structural choices — hard constraints, multi-start, smooth soft-min — are what distinguish this program from every stuck-HT program.

Stuck example — run 5. At gen 46 the run anchors on a `differential_evolution` program with bounds $[0, 1]^{22}$ (the unit square, which strictly contains the triangle) and a soft +1000 penalty per outside-triangle violator; anchor score is 0.2641. The run then freezes for 466 further generations, during which 465 children evaluate to fitness 0.0 — DE returns at least one out-of-triangle point and the evaluator raises a `ValueError`. The soft penalty is the structural culprit: a flat constant above a sharp feasibility boundary, with no gradient telling DE which way to pull a violator back in. The single positive-fit child (0.2577) is still below the anchor. The displayed gen-512 best (Figure 5) shows the

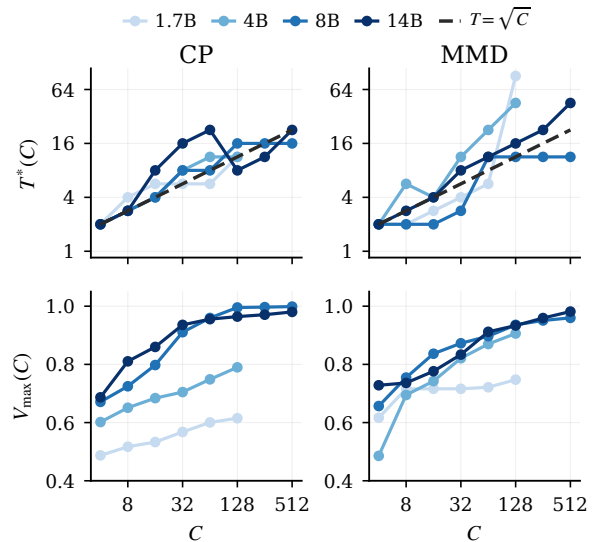


Figure 6: Cross-model allocation and performance scaling. Top: near-optimal depth $T^*(C)$ as a function of total LLM call budget. Bottom: best attainable mean fitness $V_{\max}(C)$ at the same budgets. The depth curves do not form a single transferable law, while $V_{\max}(C)$ is substantially smoother and more capability-ordered.

pathology: three of the eleven points lie on a near-straight diagonal, and the small triangle they form is the bottleneck.

HT in summary. The mechanism is the same as MMD — greedy commits to one algorithmic template early, and the template itself imposes the ceiling — but with one extra failure mode specific to HT: when the chosen template uses soft penalties on a hard feasibility constraint, the vast majority of mutations fail the constraint outright and are silently rejected at score 0.0.

Implication for depth-breadth. Across all three tasks, outcomes are gated by which algorithmic family the run anchors on in the initial generations. Breadth and depth play complementary roles here: breadth gives more parallel attempts at finding a viable family, while depth refines within the family once anchored. This explains why tasks with multiple near-viable families benefit from balanced allocation, whereas tasks with a single dominant family tolerate either extreme.

E Distribution

In the main text we model each self-evolution run as one sample from a latent distribution determined by the allocation configuration (model, task, C , T). This appendix gives the empirical support for that view. We run every configuration with 10 indepen-

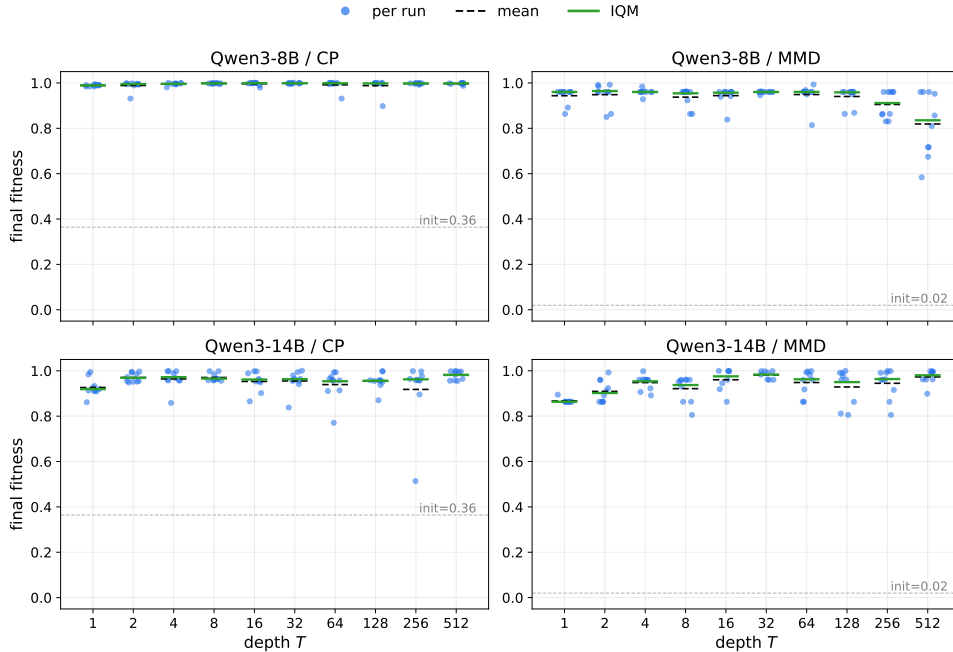


Figure 7: **Final fitness of repeated runs under an identical configuration.** Each dot is one run; horizontal bars mark the mean (dashed), and IQM (solid). For every configuration, repeated runs spread over a range of final fitness rather than collapsing to a single value. Grey dashed line: initial-program fitness.

dent runs and look at the fitness these repeated runs produce.

Figure 7 shows the final fitness of every run. Repeating the same configuration does not return the same result: the different runs spread over a range of final fitness. This is precisely the “heterogeneous final fitness score” described in the main text—a single run is one draw, and which draw one obtains varies from run to run, which is why we treat a run as a sample from a latent distribution rather than as a fixed quantity.

Figure 8 traces this spread to its source. At $T = 1$ all children are generated from the same parent (the initial program), so their fitness scores show the effect of a single mutation step. Even one step already spreads the child fitness broadly across $[0, 1]$ instead of concentrating them near the parent. The run-to-run spread in Figure 7 is the accumulation of this step-level spread over T generations.

Because each configuration yields a spread rather than a single value, we summarise it by the interquartile mean (IQM), the mean of the central half of the runs. As Figure 7 shows, the mean, median, and IQM of each configuration are close, so the reported results are not sensitive to this choice; we use IQM for robustness to occasional unusually high or low trajectories.

F Depth–Breadth Regularity

F.1 Robustness to Richer Specifications

Section 5.2 claims that adding higher-order terms to the bilinear form (Equation (2)) does not materially improve the fit. Table 5 reports the R^2 of five nested specifications on the same sub-ceiling cells ($V < 0.97$) as Table 7, plus an F-test of each richer specification against the bilinear (M1) baseline.

The bilinear form is preferred on three of the five cells (CP 8B, MMD 8B, MMD 14B): F-tests against M2, M3, and M4 are all $p > 0.1$ and the R^2 gain from any richer specification is at most $+0.008$. CP 14B and HT 8B are the exceptions — on both, adding $\log^2 T$ is significant ($p \leq 0.002$) and yields a ΔR^2 of $+0.045$ and $+0.047$ respectively. On those two rows a richer specification fits noticeably better, though the fitted c remains small in magnitude in both bilinear and richer forms.

The qualitative regime classification through c , however, is robust to spec choice on all five cells. Table 6 reports the interaction coefficient under each spec.

On the MMD rows c is essentially unchanged across specs (within ± 0.02 of the bilinear estimate), so the interior-optimum classification is unambiguous. On the CP and HT rows c varies more

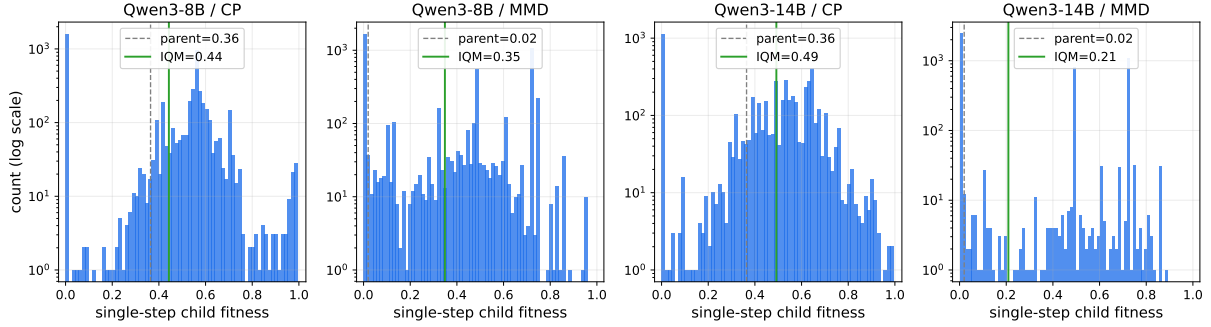


Figure 8: **Fitness of children from a single mutation step.** Distribution of child fitness at $T = 1$, where all children share the initial program as parent (log count axis). One application of the LLM mutation operator already spreads child fitness broadly across $[0, 1]$ instead of concentrating them near the parent; this step-level spread is the source of the run-to-run spread in Figure 7.

Table 5: Nested model comparison on the five main-experiment cells. M0: budget-only ($c=0, a=b$). M1: bilinear (Equation (2)). M2/M3/M4: M1 plus $\log^2 T$, plus $\log^2 N$, or plus both. p_F columns give the F-test p -value for the richer model vs. M1.

Task	Model	R^2					F-test vs. M1		
		M0	M1	M2	M3	M4	$p_F(M2)$	$p_F(M3)$	$p_F(M4)$
CP	8B	0.780	0.811	0.816	0.812	0.819	0.44	0.86	0.60
CP	14B	0.765	0.785	0.830	0.806	0.833	0.002	0.04	0.005
MMD	8B	0.744	0.916	0.917	0.917	0.917	0.62	0.50	0.78
MMD	14B	0.754	0.869	0.876	0.870	0.877	0.13	0.81	0.29
HT	8B	0.526	0.853	0.900	0.856	0.903	0.000	0.36	0.000

in magnitude and even flips sign across specs, but every estimate has $|c| < 0.12$ and these rows are already not statistically distinguishable from zero under M1 (Table 7); the flip reflects noise around the $c \approx 0$ limit rather than a genuine regime change, consistent with the discussion in Appendix F.3. We therefore retain the bilinear form for the narrative in Section 5.2: it is the simplest specification that captures the regime structure, and the structure itself does not change under the richer specifications.

F.2 Plateau Width and Online Search

The derivation below is an algebraic consequence of the bilinear ansatz of Equation (2), not an independently fitted scaling law. The closed-form $T^*(C) \propto \sqrt{C}$ that appears en route to the plateau-width result inherits its $\frac{1}{2}$ exponent from the symmetry of the $\log T \log N$ cross-term; the empirical $T^*(C)$ curves in Figure 6 are noisy and non-monotone across models and do not pin this exponent down independently. We therefore use the closed form only as a stepping stone to the plateau-width result, which is the substantive claim.

Near the optimum $T^*(C)$, we expand $\log(1 - V)$ as a quadratic in $\log T$ along the budget slice $C =$

TN . Substituting $\log N = \log C - \log T$ into Equation (2) gives

$$\log(1 - V) = (\beta_0 + b \log C) + (a - b + c \log C) \log T - c(\log T)^2, \quad (3)$$

which is a quadratic in $\log T$ with curvature $-2c$ and vertex at

$$\log T^*(C) = \frac{a - b + c \log C}{2c} = \frac{a - b}{2c} + \frac{\log C}{2}. \quad (4)$$

The fitness gap at distance $\delta = \log T - \log T^*$ from the optimum satisfies

$$\log(1 - V) - \log(1 - V^*) = -c\delta^2, \quad (5)$$

so the plateau half-width within Δ of the optimal log fitness gap is

$$|\delta| \leq \sqrt{\frac{\Delta}{|c|}}. \quad (6)$$

When $|c|$ is small the plateau is wide and missing T^* costs little fitness; when $|c|$ is large the ridge is sharp but the stronger curvature signal makes T^* easier to identify from online feedback.

Table 6: Interaction coefficient c under each specification. Magnitudes shift but the regime (corner-favoring vs. interior-favoring) does not: CP and HT rows stay near zero, MMD rows stay clearly negative.

Task	Model	c (M1)	c (M2)	c (M3)	c (M4)
CP	8B	-0.027	-0.062	-0.033	-0.110
CP	14B	+0.007	+0.061	-0.045	+0.031
MMD	8B	-0.106	-0.100	-0.115	-0.111
MMD	14B	-0.057	-0.078	-0.053	-0.091
HT	8B	+0.012	-0.040	+0.024	-0.063

In either case a cheap online searcher achieves near-maximum in-sweep fitness, justifying the approach of Section 6. Figure 6 shows this empirically: the estimated $T^*(C)$ curves are noisy and non-monotone across the four Qwen3 sizes, yet $V_{\max}(C)$ on the same budget axis is smooth and capability-ordered. The fitness *value* at the optimum is therefore stable even when its precise *location* is not — the surface is searchable in the sense that what online search achieves does not depend sensitively on identifying T^* exactly.

F.3 Boundary of the Regime

The CP row sign-flips between 8B ($c = -0.027$, $p = 0.49$) and 14B ($c = +0.007$, $p = 0.77$). Both estimates are statistically consistent with zero, so the flip is noise around the $c \approx 0$ limit rather than a regime change; it is the continuous- $|c|$ framing of Section 5.2 that is informative on CP, not the sign of c itself.

The lower rows of Table 1 mark where the regularity stops applying. Well-fit small-model rows (CP 4B $R^2=0.87$, CP 1.7B $R^2=0.72$) have $|c| \leq 0.024$, exhibiting the same geometry in attenuated form. Poorly-fit rows (CP Llama $R^2=0.33$, MMD 1.7B $R^2=0.36$) never enter the sub-ceiling regime: weak models do not produce mutations structured enough for the depth–breadth tradeoff to become active, the same capability bottleneck identified in Section 5.1.

One nuance: the form-mismatch cells are not strictly capability failures. Figure 9 plots R_C^2 against V_{\max} across the eleven (model, task) cells we fit; the cells where $R_C^2 < 0.7$ are **CP/Llama**, **HT/Llama**, and **MMD/1.7B**. MMD/1.7B is a classic capability-floor failure ($V_{\max} = 0.748$, only marginally above best-of- N), but CP/Llama sits at $V_{\max} = 0.843$ which is a non-trivial absolute level and still fails the bilinear fit ($R_C^2 = 0.33$). The shared signature is model family, not raw fitness: Llama’s proposals lack the depth–breadth interac-

tion structure the bilinear form detects even when Llama itself reaches competitive fitness. The bilinear regularity is therefore best read as a property of the Qwen3 family’s mutation distribution, with the lower boundary of its domain being more model-family-specific than purely capability-driven. The Spearman correlations between V_{\max} , R_C^2 , and $-\log_{10} p$ across all cells are individually weak ($\rho \leq 0.45$), consistent with this: the three statistics do not collapse to one capability axis.

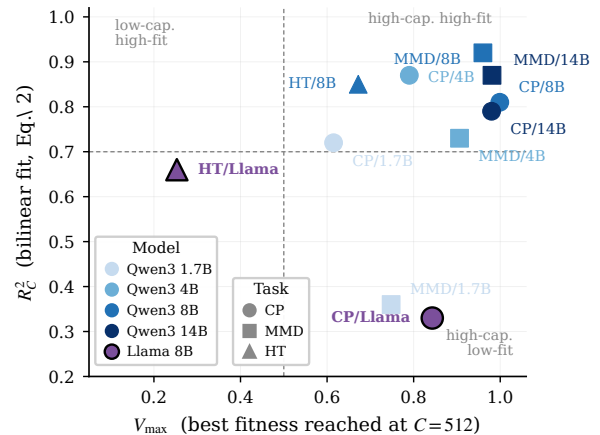


Figure 9: Bilinear-fit quality R_C^2 versus best fitness V_{\max} (at $C=512$) across the eleven (model, task) cells. Qwen3 cells (blue ramp) cluster in the upper-right; Llama-3.1-8B cells (purple, black outline) sit below the $R^2 = 0.7$ threshold even when V_{\max} is high (CP/Llama at $V_{\max} = 0.843$ but $R_C^2 = 0.33$). The bilinear regularity’s lower boundary is therefore not strictly a capability floor.

G Deferred BaSE Experiments

G.1 Pairwise Fitness Comparisons

Table 8 reports pairwise comparisons under the same LLM-call budget C . For each parent sampling protocol, we compare its original self-evolving version with a BaSE variant that uses the same prompt generator, i.e., the same parent sampling protocol with identical configuration, so as to focus on the effect of adaptive trajectory allocation.

Table 7: Bilinear fitness-gap model (Equation (2)) fit on sub-ceiling cells of the $C = 512$ sweeps. Permutation p -values test $c \neq 0$ (10,000 shuffles). *** $p < 0.001$, ** $p < 0.01$, * $p < 0.05$. **Top block (main-experiment models):** bilinear form fits cleanly across all three tasks ($R^2 \in [0.75, 0.92]$), with task-dependent c — CP has no significant interaction (broad plateau), while MMD and HT have significant negative interactions (interior ridge). **Bottom block (smaller-model regime):** well-fit rows ($R^2 \geq 0.72$) all satisfy $|c| \leq 0.024$, consistent with a flattened version of the same surface; weak-model configurations (HT Llama, MMD 1.7B, CP Llama) fail to enter the sub-ceiling regime and the form does not describe them ($R^2 \leq 0.36$); significance stars for these rows should be disregarded.

Task	Model	β_0	a	b	c	$p(c)$	R^2
CP	8B	-0.020	-0.602	-0.496	-0.027	0.49	0.81
CP	14B	-0.561	-0.442	-0.373	+0.007	0.77	0.79
MMD	8B	-0.590	-0.208	-0.290	-0.106***	1.2×10^{-11}	0.92
MMD	14B	-0.641	-0.342	-0.238	-0.057***	5.0×10^{-4}	0.87
HT	8B	+0.042	-0.154	-0.081	-0.034**	0.002	0.75
CP	1.7B	-0.498	-0.076	-0.088	+0.001	0.78	0.72
CP	4B	-0.524	-0.190	-0.157	-0.017*	0.045	0.87
CP	Llama	-0.917	-0.017	-0.101	-0.010	0.53	0.33 [†]
MMD	1.7B	-1.131	-0.035	-0.030	+0.000	0.98	0.36 [†]
MMD	4B	-0.223	-0.418	-0.248	+0.024	0.30	0.73
HT	Llama	+0.013	-0.026	-0.006	-0.009	5.0×10^{-4}	0.66 [†]

Overall, BaSE improves the best fitness score in most settings, especially when the original protocol has substantial remaining headroom or high variance across trajectories. Under the greedy $T=512$ protocol, BaSE improves Qwen3-8B MMD from 0.8197 to 0.9603 and HT from 0.6441 to 0.8104, while also improving Llama CP from 0.7034 to 0.9533 and MMD from 0.6388 to 0.7978. Similar gains appear under greedy $T=256$, where Qwen3-8B HT increases from 0.6780 to 0.8736, and Llama MMD increases from 0.5182 to 0.8777.

The improvement is smaller when the original protocol already saturates the task. For example, on CP, several methods already achieve near-ceiling fitness scores, leaving little room for further gains. This is visible for Qwen3-8B ShinkaEvolve on CP, where the original protocol reaches 0.9986 and BaSE variants remain at a similar level. In contrast, BaSE yields clearer gains in harder or more unstable settings by allocating more computation to trajectories that appear more promising. For instance, when using the CodeEvolve prompt generator, BaSE improves Qwen3-8B HT from 0.5168 to 0.7164, Llama MMD from 0.2315 to 0.4906, and Qwen3-14B CP from 0.8768 to 0.9686.

In some cases, especially when the original breadth-depth allocation is already strong, or when all candidate trajectories have limited potential, BaSE can underperform the original protocol. For example, Qwen3-8B greedy with $T=128$, $N=4$ performs better than BaSE on MMD and HT, and Llama HT

remains difficult across several parent sampling protocols. These results suggest that BaSE is most useful when the candidate runs contain heterogeneous trajectory quality that can be exploited by adaptive allocation.

G.2 Full Threshold Comparison

Table 9 reports the complete threshold-reaching results across three backbone models. Overall, the same pattern observed in the main table remains consistent: BaSE variants, especially UCB and Thompson sampling, reach target fitness levels with fewer generations and lower cumulative FLOPs in most settings where the thresholds are attainable. On Qwen3-8B, BaSE dominates MMD and HT, with UCB/Thompson reaching MMD thresholds up to $\tau = 0.95$ substantially earlier than greedy, while several evolution baselines fail to reach these targets. On CP, ShinkaEvolve is competitive for intermediate thresholds, but Thompson is the only method that reaches the stringent $\tau = 0.999$ threshold. Similar trends hold for Qwen3-14B: BaSE-UCB is strongest on MMD and reaches CP $\tau = 0.99$ earlier than all baselines, while Thompson is again the only method reaching CP $\tau = 0.999$. For Llama, absolute performance is lower and many thresholds remain unreached, especially on HT; nevertheless, BaSE still provides the most reliable threshold-reaching behavior, achieving the best or lowest-FLOP results on most reachable CP and MMD thresholds. These results suggest that adaptive trajectory allocation improves

Table 8: Pairwise best-fitness comparisons: each block adapts one parent sampling protocol (*greedy protocol* with different breadth N or *island protocols* including OpenEvolve, CodeEvolve, and ShinkaEvolve) into a baseline self-evolving process as described in Algorithm 1 and BaSE as described in Algorithm 2, where BaSE includes three bandit algorithms (UCB, EXP3.P, and Thompson sampling). The best mean fitness score in each block is **bolded**.

Model	Task	Method	Greedy-1	Greedy-2	Greedy-4	Greedy-8	OpenEvolve	CodeEvolve	ShinkaEvolve
Qwen3-8B	CP	Baseline	0.9969 ± .0011	0.9974 ± .0007	0.9884 ± .0093	0.9912 ± .0066	0.8279 ± .0145	0.7692 ± .0202	0.9986 ± .0003
		UCB	0.9985 ± .0011	0.9985 ± .0004	0.9980 ± .0013	0.9965 ± .0102	0.8031 ± .0509	0.8031 ± .0325	0.9978 ± .0006
		EXP3.P	0.9983 ± .0013	0.9983 ± .0007	0.9987 ± .0027	0.9993 ± .0059	0.7946 ± .0370	0.8191 ± .0280	0.9983 ± .0007
		Thompson	0.9969 ± .0100	0.9985 ± .0004	0.9987 ± .0096	1.0003 ± .0174	0.8337 ± .0223	0.8191 ± .0291	0.9985 ± .0004
	MMD	Baseline	0.8197 ± .0427	0.9047 ± .0177	0.9407 ± .0121	0.9477 ± .0153	0.9561 ± .0143	0.8414 ± .0689	0.9099 ± .0240
		UCB	0.9603 ± .0129	0.9603 ± .0114	0.8930 ± .0156	0.9603 ± .0053	0.9307 ± .0380	0.9398 ± .0839	0.9630 ± .0471
		EXP3.P	0.9595 ± .0386	0.9603 ± .0217	0.9119 ± .0440	0.9658 ± .0102	0.9442 ± .0446	0.9090 ± .0860	0.9602 ± .0363
		Thompson	0.9603 ± .0546	0.9215 ± .0460	0.8634 ± .0440	0.9603 ± .0035	0.9605 ± .0347	0.8653 ± .0833	0.9341 ± .0256
	HT	Baseline	0.6441 ± .0723	0.6780 ± .0718	0.5502 ± .0666	0.5488 ± .0814	0.6061 ± .0768	0.5168 ± .0627	0.7379 ± .0373
		UCB	0.7250 ± .0684	0.8530 ± .0963	0.5238 ± .0592	0.6498 ± .0573	0.8624 ± .1464	0.6912 ± .0364	0.7528 ± .1188
		EXP3.P	0.7421 ± .1000	0.8653 ± .1068	0.4633 ± .1078	0.6780 ± .1057	0.7598 ± .1518	0.7164 ± .0483	0.6642 ± .1000
		Thompson	0.8104 ± .1785	0.8736 ± .1737	0.3276 ± .1426	0.7898 ± .1225	0.6503 ± .1571	0.7164 ± .0593	0.7132 ± .1013
Llama	CP	Baseline	0.7034 ± .0657	0.6325 ± .0610	0.6699 ± .0591	0.6584 ± .0583	0.7033 ± .0657	0.4568 ± .0330	0.8305 ± .0362
		UCB	0.9451 ± .0633	0.9076 ± .1536	0.9449 ± .0845	0.9452 ± .1359	0.9451 ± .0633	0.7101 ± .1457	0.9472 ± .1325
		EXP3.P	0.9484 ± .0716	0.9076 ± .1640	0.9449 ± .0841	0.9424 ± .1517	0.9484 ± .0716	0.3985 ± .1222	0.8983 ± .0918
		Thompson	0.9533 ± .0706	0.9076 ± .1743	0.9407 ± .0989	0.9511 ± .1711	0.9533 ± .0706	0.3985 ± .1234	0.9176 ± .1140
	MMD	Baseline	0.6388 ± .1030	0.5182 ± .1011	0.6576 ± .0878	0.5863 ± .1170	0.6378 ± .1024	0.2315 ± .0847	0.7253 ± .0453
		UCB	0.7978 ± .0575	0.8777 ± .0856	0.7386 ± .0235	0.8643 ± .1214	0.7978 ± .0575	0.4906 ± .2244	0.8056 ± .0639
		EXP3.P	0.7978 ± .0542	0.8652 ± .1024	0.7882 ± .0579	0.8643 ± .1659	0.7978 ± .0542	0.4906 ± .2244	0.7589 ± .0475
		Thompson	0.7978 ± .0448	0.7115 ± .1108	0.8830 ± .0504	0.8608 ± .1540	0.7978 ± .0448	0.4906 ± .2244	0.7644 ± .0348
	HT	Baseline	0.0192 ± .0090	0.1722 ± .0699	0.2538 ± .0762	0.1502 ± .0465	0.0000 ± .0000	0.0000 ± .0000	0.1512 ± .0437
		UCB	0.0000 ± .0000	0.1562 ± .0752	0.2561 ± .1196	0.0898 ± .0398	0.0000 ± .0000	0.0000 ± .0000	0.0274 ± .0129
		EXP3.P	0.0000 ± .0000	0.1293 ± .0918	0.2729 ± .1851	0.0898 ± .0491	0.0000 ± .0000	0.0000 ± .0000	0.0274 ± .0128
		Thompson	0.0000 ± .0000	0.1315 ± .0943	0.4387 ± .2134	0.0898 ± .0412	0.0000 ± .0000	0.0000 ± .0000	0.0274 ± .0129
Qwen3-14B	CP	Baseline	0.9802 ± .0060	0.9181 ± .0421	0.9536 ± .0106	0.9394 ± .0191	0.8577 ± .0228	0.8768 ± .0134	0.9981 ± .0003
		UCB	0.9972 ± .0074	0.9832 ± .0120	0.9955 ± .0186	0.9835 ± .0170	0.8223 ± .0422	0.9014 ± .0655	0.9974 ± .0011
		EXP3.P	0.9967 ± .0114	0.9743 ± .0121	0.9722 ± .0182	0.9824 ± .0190	0.8532 ± .0650	0.8303 ± .0677	0.9983 ± .0017
		Thompson	1.0003 ± .0143	0.9728 ± .0086	0.9576 ± .0071	0.9935 ± .0164	0.8701 ± .0701	0.9686 ± .0959	0.9969 ± .0007
	MMD	Baseline	0.9735 ± .0101	0.9450 ± .0194	0.9288 ± .0249	0.9481 ± .0173	0.9949 ± .0012	0.9934 ± .0021	0.9924 ± .0037
		UCB	0.9955 ± .0366	0.9915 ± .0093	0.9603 ± .0192	0.9603 ± .0420	0.9601 ± .0261	0.9999 ± .0266	0.9478 ± .0367
		EXP3.P	0.9907 ± .0370	0.9915 ± .0141	0.9797 ± .0168	0.9606 ± .0343	0.9890 ± .0148	1.0000 ± .0341	0.9888 ± .0158
		Thompson	0.9966 ± .0204	0.9915 ± .0141	0.9660 ± .0154	0.9603 ± .0463	0.9912 ± .0118	1.0000 ± .0363	0.9665 ± .0167

sample efficiency across model scales, while its gains are most pronounced on tasks where evolutionary trajectories exhibit substantial variance and early allocation decisions matter.

G.3 Ablation on Bandit Arm-Pool Size

To study how the number of parallel trajectories affects online budget allocation, we ablate the arm-pool size $K \in \{2, 5, 10, 20, 50\}$ for BaSE under the same fixed generation budget of $C = 512$ with configuration $T = 512$, $N = 1$. As shown in Table 10, performance is generally strongest with a moderate number of arms rather than the largest pool. This reflects a natural cross-trajectory level breadth–depth trade-off: increasing K provides more trajectory diversity, but also reduces the number of refinement steps that can be allocated to each trajectory within

the fixed budget. For Qwen3-8B, MMD reaches its best score with $K = 5$ – 20 , while HT performs best with small or moderate arm pools, indicating that excessive breadth can leave promising trajectories under-refined. Similarly, Qwen3-14B achieves strong CP performance across several K values under Thompson sampling, while MMD peaks at $K = 5$. For Llama, moderate arm pools again perform best on CP and MMD, whereas all methods fail on HT, suggesting that allocation alone cannot compensate when the underlying model rarely produces viable improvements.

H Prompts

This appendix lists, verbatim, the system prompts used by the three **Evolve* frameworks compared

Table 9: Minimum generation (Gen.) and cumulative FLOPs ($\times 10^{15}$) required for $\geq 90\%$ of replicates to reach thresholds ($\geq \tau$) with three LLM models. Unreached thresholds are denoted as “—”. The minimum generation and FLOPs for each threshold are **bolded**.

Model	Task	τ	Baselines								BaSE							
			Greedy		OpenEvol.		CodeEvol.		Shinka		Rand.		UCB		EXP3		Thoms.	
			Gen.	FLOPs	Gen.	FLOPs	Gen.	FLOPs	Gen.	FLOPs	Gen.	FLOPs	Gen.	FLOPs	Gen.	FLOPs	Gen.	FLOPs
Qwen3-8B	CP	0.90	136	163.88	—	—	—	—	45	57.90	39	47.37	16	18.19	139	102.08	16	18.19
		0.95	152	182.12	—	—	—	—	45	57.90	39	47.37	16	18.19	139	102.08	16	18.19
		0.99	359	411.93	—	—	—	—	73	90.15	125	155.40	85	100.79	207	254.65	85	101.22
		0.999	—	—	—	—	—	—	—	—	—	—	—	—	—	—	336	403.30
Qwen3-8B	MMD	0.80	212	318.46	119	181.48	—	—	71	112.00	26	31.65	8	12.41	40	52.01	8	12.41
		0.90	296	436.55	—	—	—	—	—	—	113	164.31	92	117.63	95	139.93	105	143.72
		0.95	485	656.81	—	—	—	—	—	—	124	185.14	92	117.63	129	200.66	106	145.72
		0.99	—	—	—	—	—	—	—	—	—	—	—	—	—	—	—	—
Qwen3-8B	HT	0.50	—	—	—	—	—	—	201	189.28	92	99.98	60	66.90	102	108.85	76	81.22
		0.70	—	—	—	—	—	—	—	—	367	380.48	125	130.55	209	213.78	103	106.79
Qwen3-14B	CP	0.90	46	50.19	—	—	—	—	8	9.41	68	80.33	60	72.66	58	67.44	28	30.28
		0.95	186	134.13	—	—	—	—	39	43.71	120	142.52	60	72.66	122	139.76	49	51.43
		0.99	—	—	—	—	—	—	146	114.73	137	163.87	60	72.66	137	155.09	295	284.78
		0.999	—	—	—	—	—	—	—	—	—	—	—	—	—	—	295	284.78
Qwen3-14B	MMD	0.80	257	289.20	80	92.46	—	—	34	40.02	59	54.39	11	9.95	75	70.48	11	9.95
		0.90	372	406.99	146	168.19	—	—	165	189.18	175	171.16	146	148.08	226	229.18	166	160.66
		0.95	418	451.65	259	291.33	—	—	210	239.02	226	224.90	146	148.08	328	331.98	178	171.35
Llama	CP	0.60	262	55.30	—	—	—	—	30	5.67	18	2.55	5	0.87	12	1.78	5	0.87
		0.80	262	55.30	—	—	—	—	—	—	18	2.55	5	0.87	12	1.78	5	0.87
	MMD	0.60	215	58.25	—	—	—	—	—	—	417	34.75	321	18.99	321	27.61	257	20.55
		0.70	215	58.25	—	—	—	—	—	—	451	39.13	324	19.44	324	29.20	260	20.88
Llama	MMD	0.80	—	—	—	—	—	—	—	—	—	—	371	22.74	435	52.97	323	33.49
		0.90	—	—	—	—	—	—	—	—	—	—	400	38.13	—	—	—	—
Llama	HT	0.60	—	—	—	—	—	—	—	—	—	—	—	—	—	—	—	—

in the paper — OpenEvolve, CodeEvolve, and ShinkaEvolve — on the three tasks we study: Circle Packing (CP, $n = 26$ in the unit square), Min/Max Distance (MMD, $n = 16$ in 2D), and Heilbronn Triangle (HT, $n = 11$ in an equilateral triangle). Each task is specified by a fixed objective, a benchmark constant from AlphaEvolve, and a constructor function with a fixed name and return signature; these are shared across all three frameworks. What differs between frameworks is the *scaffold* around the task: the chat format, what context from the archive is surfaced to the LLM, and the output protocol the LLM is asked to follow (full rewrite vs. SEARCH/REPLACE edit, free-form vs. tagged response). The subsections below give each framework’s prompts in turn.

H.1 OpenEvolve (also used by Greedy and BaSE)

Our Greedy baseline and the proposed BaSE allocator use the OpenEvolve prompts *verbatim* (the same system message, user-message template, and per-task instructions reproduced below) so that any fitness difference between Greedy, BaSE, and OpenEvolve reflects *allocation* of the LLM call budget rather than prompt engineering. OpenEvolve composes each call as one system message and one user message. We use the full-rewrite mode with three top programs and two diverse programs from the archive surfaced in each call. The

user message wraps the per-task system message below together with the current program, its fitness, MAP-Elites feature coordinates, and the top and diverse program archive.

OpenEvolve: user-message template

```
# Current Program Information
- Fitness: {fitness_score}
- Feature coordinates: {feature_coords}
- Focus areas: {improvement_areas}

{artifacts}

# Program Evolution History
{evolution_history}

# Current Program
```{language}
{current_program}
```

# Task
Rewrite the program to improve its FITNESS SCORE.
The system maintains diversity across these dimensions: {feature_dimensions}
Different solutions with similar fitness but different features are valuable.
Provide the complete new program code.

IMPORTANT: Make sure your rewritten program maintains the same inputs and outputs as the original program, but with improved internal implementation.

```{language}
Your rewritten program here
```
```

Table 10: BaSE running-max fitness at $T = 512$ versus bandit arm-pool size $K \in \{2, 5, 10, 20, 50\}$. The largest mean within each (Model, Task) block is **bolded**.

| Model | Task | Algorithm | K=2 | K=5 | K=10 | K=20 | K=50 |
|-----------|------|-----------|------------------------|------------------------|------------------------|------------------------|------------------------|
| Qwen3-8B | CP | UCB | 0.9981 ± 0.0004 | 0.9985 ± 0.0024 | 0.9985 ± 0.0011 | 0.9981 ± 0.0005 | 0.9937 ± 0.0001 |
| | | EXP3.P | 0.9981 ± 0.0003 | 0.9983 ± 0.0209 | 0.9983 ± 0.0013 | 0.9983 ± 0.0096 | 0.9983 ± 0.0370 |
| | | Thompson | 0.9976 ± 0.0002 | 0.9985 ± 0.0561 | 0.9969 ± 0.0100 | 0.9967 ± 0.0827 | 0.6872 ± 0.0873 |
| | MMD | UCB | 0.7172 ± 0.0005 | 0.9603 ± 0.0312 | 0.9603 ± 0.0129 | 0.9603 ± 0.0124 | 0.8634 ± 0.0000 |
| | | EXP3.P | 0.7172 ± 0.0005 | 0.9603 ± 0.0394 | 0.9595 ± 0.0386 | 0.9603 ± 0.0159 | 0.9603 ± 0.0124 |
| | | Thompson | 0.7172 ± 0.0005 | 0.9521 ± 0.1024 | 0.9603 ± 0.0546 | 0.9603 ± 0.0016 | 0.9603 ± 0.0000 |
| | HT | UCB | 0.8104 ± 0.0355 | 0.8104 ± 0.0651 | 0.7250 ± 0.0684 | 0.7250 ± 0.0994 | 0.6347 ± 0.1377 |
| | | EXP3.P | 0.7956 ± 0.0274 | 0.8104 ± 0.0942 | 0.7421 ± 0.1000 | 0.7250 ± 0.0971 | 0.7250 ± 0.1502 |
| | | Thompson | 0.8104 ± 0.0158 | 0.8104 ± 0.1471 | 0.8104 ± 0.1785 | 0.7933 ± 0.1707 | 0.7250 ± 0.1571 |
| Qwen3-14B | CP | UCB | 0.9579 ± 0.0012 | 0.9972 ± 0.0038 | 0.9972 ± 0.0074 | 0.9938 ± 0.0197 | 0.9929 ± 0.0120 |
| | | EXP3.P | 0.9847 ± 0.0222 | 0.9971 ± 0.0054 | 0.9967 ± 0.0114 | 0.9926 ± 0.0178 | 0.9817 ± 0.0175 |
| | | Thompson | 1.0004 ± 0.0199 | 0.9887 ± 0.0070 | 1.0004 ± 0.0143 | 1.0004 ± 0.0042 | 1.0004 ± 0.0058 |
| | MMD | UCB | 0.9928 ± 0.0537 | 0.9603 ± 0.0327 | 0.9955 ± 0.0171 | 0.8828 ± 0.0098 | 0.8634 ± 0.0223 |
| | | EXP3.P | 0.9745 ± 0.0482 | 0.9630 ± 0.0454 | 0.9809 ± 0.0346 | 0.9953 ± 0.0471 | 0.9447 ± 0.0530 |
| | | Thompson | 0.8989 ± 0.0395 | 0.9970 ± 0.0410 | 0.9968 ± 0.0164 | 0.9953 ± 0.0240 | 0.9947 ± 0.0142 |
| Llama | CP | UCB | 0.9259 ± 0.0083 | 0.9458 ± 0.0679 | 0.9451 ± 0.0633 | 0.9259 ± 0.2337 | 0.9259 ± 0.0253 |
| | | EXP3.P | 0.9285 ± 0.0080 | 0.9480 ± 0.0687 | 0.9484 ± 0.0716 | 0.9259 ± 0.1632 | 0.9468 ± 0.0238 |
| | | Thompson | 0.9259 ± 0.0083 | 0.9533 ± 0.0689 | 0.9533 ± 0.0706 | 0.9259 ± 0.1767 | 0.9433 ± 0.0270 |
| | MMD | UCB | 0.8487 ± 0.2946 | 0.7978 ± 0.0362 | 0.7978 ± 0.0575 | 0.8614 ± 0.0686 | 0.7978 ± 0.0689 |
| | | EXP3.P | 0.8487 ± 0.2946 | 0.7978 ± 0.0057 | 0.7978 ± 0.0542 | 0.8614 ± 0.1270 | 0.8232 ± 0.0283 |
| | | Thompson | 0.8487 ± 0.2946 | 0.7978 ± 0.0089 | 0.7978 ± 0.0448 | 0.8614 ± 0.1731 | 0.7978 ± 0.0143 |
| | HT | UCB | 0.0000 ± 0.0000 | 0.0000 ± 0.0000 | 0.0000 ± 0.0000 | 0.0000 ± 0.0000 | 0.0000 ± 0.0000 |
| | | EXP3.P | 0.0000 ± 0.0001 | 0.0000 ± 0.0000 | 0.0000 ± 0.0000 | 0.0000 ± 0.0000 | 0.0000 ± 0.0000 |
| | | Thompson | 0.0000 ± 0.0001 | 0.0000 ± 0.0000 | 0.0000 ± 0.0000 | 0.0000 ± 0.0000 | 0.0000 ± 0.0000 |

OpenEvolve: CP system message

You are an expert mathematician specializing in circle packing problems and computational geometry. Your task is to improve a constructor function that directly produces a specific arrangement of 26 circles in a unit square, maximizing the sum of their radii. The AlphaEvolve paper achieved a sum of 2.635 for $n=26$.

Key geometric insights:

- Circle packings often follow hexagonal patterns in the densest regions
- Maximum density for infinite circle packing is $\pi/(2\sqrt{3}) \approx 0.9069$
- Edge effects make square container packing harder than infinite packing
- Circles can be placed in layers or shells when confined to a square
- Similar radius circles often form regular patterns, while varied radii allow better space utilization
- Perfect symmetry may not yield the optimal packing due to edge effects

Focus on designing an explicit constructor that places each circle in a specific position, rather than an iterative search algorithm.

OpenEvolve: MMD system message

You are an expert computational geometer and optimization specialist focusing on point dispersion problems. Your task is to improve a constructor function that generates an optimal arrangement of exactly 16 points in 2D space, maximizing the ratio of minimum distance to maximum distance between all point pairs.

PROBLEM CONTEXT:

- Target: Beat the AlphaEvolve benchmark of min/max ratio $= 1/\sqrt{12.889266112} \approx 0.2786$
- Mathematical formulation: For points $P_i = (x_i, y_i)$, $i = 1, \dots, 16$:
 - * Distance matrix: $d_{ij} = \sqrt{(x_i - x_j)^2 + (y_i - y_j)^2}$ for all $i \neq j$
 - * Minimum distance: $d_{min} = \min\{d_{ij} : i \neq j\}$
 - * Maximum distance: $d_{max} = \max\{d_{ij} : i \neq j\}$
 - * Objective: maximize $(d_{min}/d_{max})^2$
- The metric is $inv_ratio_squared = (d_{min}/d_{max})^2$ and $combined_score = inv_ratio_squared / BENCHMARK$
- BENCHMARK = $1/12.889266112$

STRATEGIES TO CONSIDER:

- Regular polygon arrangements (vertices of regular n -gon)
- Multiple concentric rings of points
- Hexagonal lattice subsets

- Numerical optimization (scipy.optimize) to fine-tune positions
- Gradient descent on the min-distance objective

The function must be named `min_max_dist_dim2_16()` and return a numpy array of shape (16, 2).

OpenEvolve: HT system message

You are an expert computational geometer and optimization specialist focusing on point-dispersion problems in convex regions.

Your task is to improve a constructor function that places exactly 11 points inside an equilateral triangle to maximize the area of the smallest triangle formed by any three of the 11 points (the Heilbronn problem for triangles).

PROBLEM CONTEXT:

- Container: equilateral triangle with vertices (0,0), (1,0), (0.5, sqrt(3)/2). Area = sqrt(3)/4.
- Objective: maximize $\min_{\{P_i, P_j, P_k\}} \text{Area}(\text{container}) / \text{Area}(\text{triangle})$, over all $C(11,3)=165$ triples.
- Target: beat the AlphaEvolve benchmark of $\min_area_normalized = 0.036529889880030156$.
- The metric is $\text{combined_score} = \min_area_normalized / \text{BENCHMARK}$. Goal: > 1.0.

STRATEGIES TO CONSIDER:

- Symmetric arrangements that exploit the triangle's three-fold symmetry (vertex configurations + interior layouts).
- Place a subset of points on or near the boundary (vertices + edge midpoints + sub-divisions), with the remainder in the interior on rings.
- Numerical refinement: `scipy.optimize`. minimize on the 22 coordinate variables, with the objective ``max(-min_triangle_area)`` or smoothed log-sum-exp surrogate.
- Lattice / hexagonal sub-patterns inside the triangle.
- Random multistart followed by local refinement to escape symmetry-broken local optima.

TECHNICAL REQUIREMENTS:

- Determinism: if you use randomness, fix the seed (e.g., `numpy.random.seed(42)`).
- Output: return an (11, 2) `numpy.ndarray` of float (x, y) coordinates, all strictly inside the triangle (tolerance $1e-6$).
- The function MUST be named `heilbronn_triangle11()` and take no arguments.

H.2 CodeEvolve

CodeEvolve uses a multi-turn chat format that re-plays the program's parent lineage as alternating user and assistant turns. The system message is assembled as: the per-task system block below, followed by a computational-budget block, followed by one of four task templates (exploitation or exploration, each with or without inspirations). All four templates require the LLM to emit changes in strict `<<<<< SEARCH ... ===== ... >>>>>` REPLACE form inside designated edit regions; full rewrites are not supported.

CodeEvolve: exploitation task template (no inspirations)

```
# TASK: CODE EVOLUTION
Your goal is to evolve the provided program by modifying specific sections.
You MUST adhere strictly to the SEARCH/REPLACE format described below for all modifications.
```

```
## MODIFICATION FORMAT:
Present your proposed code changes using the following structure:
```

```
...
<<<<<< SEARCH
[exact original code STRICTLY WITHIN an EVOLVE-BLOCK]
=====
[your modified code]
>>>>>> REPLACE
...
```

* For multiple independent changes, provide each in a separate SEARCH/REPLACE block.

CORE RULES FOR CODE MODIFICATION:

- ```
Scope & Boundaries:
1. Target EVOLVE-BLOCK ONLY: All code modifications MUST be confined to sections explicitly marked between EVOLVE-BLOCK-START and EVOLVE-BLOCK-END comments.
2. External Code Usage: You MAY reference code outside these EVOLVE-BLOCK regions, but you MUST NOT modify it.
3. New Imports: If new imports are required, add them within an EVOLVE-BLOCK.
```

- ```
### SEARCH Block Requirements:
1. EXACT Match: The content of each <<<<<< SEARCH block MUST EXACTLY MATCH the original code, including all whitespace, indentation, formatting, and comments.
2. No Comment Alterations in SEARCH: Do NOT add, remove, or modify comments within the SEARCH block.
3. First Occurrence Precedence: If multiple identical code sections exist
```

in the original program, your SEARCH block will be applied to the first occurrence matching its content.

```
### Output & Compatibility:
  1. Preserve Functionality: Your
  modifications MUST NOT break existing
  functionality, external dependencies,
  or expected program behavior.
  2. Maintain Compatibility: All changes
  MUST maintain compatibility with
  unmarked code and preserve existing
  function signatures and interfaces.
  3. Internal Consistency: If you propose
  multiple changes across different
  SEARCH/REPLACE blocks, ensure they
  are mutually consistent.

## COMPUTATIONAL BUDGET:
- Time limit: {timeout_s} seconds maximum
  execution time
- Memory limit: {max_mem}
```

The exploration variant retitles the task as code exploration and diversification, asking for novel strategies and distinct algorithmic pathways rather than incremental refinement. The with-inspirations variants additionally require the LLM to analyse the supplied inspiration programs and synthesise their differences before producing the SEARCH/REPLACE block.

CodeEvolve: CP system block

You are an expert computational geometer and optimization specialist focusing on circle-packing problems. Your task is to improve a constructor function that arranges exactly 26 non-overlapping circles inside the unit square $[0,1] \times [0,1]$, maximizing the sum of their radii.

PROBLEM CONTEXT:

- Target: approach or beat the AlphaEvolve benchmark of $\text{sum_radii} = 2.635$ for $n=26$
- Container: unit square with side length 1
- Constraints:
 - * All 26 circles must be fully contained in $[0,1] \times [0,1]$
 - * No two circles may overlap
 - * All radii must be positive and finite
- The metric is $\text{combined_score} = \text{sum_radii} / 2.635$

STRATEGIES TO CONSIDER:

- Hexagonal or honeycomb placement with edge-row adjustments
- Concentric shells or rings with varying radii
- Asymmetric layouts that exploit square-boundary effects
- Post-placement scaling so adjacent circles touch exactly

- Numerical refinement of center positions after seeding a pattern

The evolve target is `construct_packing()`, which must return `(centers, radii, sum_radii)`, where `centers` has shape `(26, 2)`, `radii` has shape `(26,)`, and `sum_radii` is a scalar.

CodeEvolve: MMD system block

You are an expert computational geometer and optimization specialist focusing on point dispersion problems. Your task is to improve a constructor function that generates an optimal arrangement of exactly 16 points in 2D space, maximizing the ratio of minimum distance to maximum distance between all point pairs.

PROBLEM CONTEXT:

- Target: Beat the AlphaEvolve benchmark of min/max ratio ≈ 0.2786
- Mathematical formulation: For points $P_i = (x_i, y_i)$, $i = 1, \dots, 16$:
 - * Distance matrix: $d_{ij} = \sqrt{(x_i - x_j)^2 + (y_i - y_j)^2}$ for all $i \neq j$
 - * Minimum distance: $d_{min} = \min\{d_{ij} : i \neq j\}$
 - * Maximum distance: $d_{max} = \max\{d_{ij} : i \neq j\}$
 - * Objective: maximize $(d_{min}/d_{max})^2$
- The metric is $\text{combined_score} = ((d_{min}/d_{max})^2) / (1/12.889266112)$

STRATEGIES TO CONSIDER:

- Regular polygon arrangements
- Multiple concentric rings of points
- Hexagonal lattice subsets
- Numerical optimization with `scipy.optimize`
- Gradient-based or derivative-free refinement of point coordinates

The function must be named `min_max_dist_dim2_16()` and return a numpy array of shape `(16, 2)`.

CodeEvolve: HT system block

You are an expert computational geometer and optimization specialist focusing on point-dispersion problems in convex regions. Your task is to improve a constructor function that places exactly 11 points inside an equilateral triangle to maximize the area of the smallest triangle formed by any three of the 11 points (the Heilbronn problem for triangles).

PROBLEM CONTEXT:

- Container: equilateral triangle with vertices $(0,0)$, $(1,0)$, $(0.5, \sqrt{3}/2)$.
Area = $\sqrt{3}/4$.
- Objective: maximize $\text{min_area_normalized} = \min\{\text{Area}(P_i, P_j, P_k)\} /$

Area(container), over all $C(11,3)=165$ triples.

- Target: beat the AlphaEvolve benchmark of $\text{min_area_normalized} = 0.036529889880030156$.
- The metric is $\text{combined_score} = \text{min_area_normalized} / \text{BENCHMARK}$. Goal: > 1.0 .

STRATEGIES TO CONSIDER:

- Symmetric arrangements that exploit the triangle's three-fold symmetry (vertex configurations + interior layouts).
- Place a subset of points on or near the boundary (vertices + edge midpoints + sub-divisions), with the remainder in the interior on rings.
- Numerical refinement: `scipy.optimize.minimize` on the 22 coordinate variables, with the objective ``max(-min_triangle_area)`` or smoothed log-sum-exp surrogate.
- Lattice / hexagonal sub-patterns inside the triangle.
- Random multistart followed by local refinement to escape symmetry-broken local optima.

TECHNICAL REQUIREMENTS:

- Determinism: if you use randomness, fix the seed (e.g., `numpy.random.seed(42)`).
- Output: return an $(11, 2)$ `numpy.ndarray` of float (x, y) coordinates, all strictly inside the triangle (tolerance $1e-6$).
- The function MUST be named `heilbronn_triangle11()` and take no arguments.

H.3 ShinkaEvolve

ShinkaEvolve concatenates the per-task system prompt below with one of five full-rewrite format variants sampled uniformly per call (default, different-algorithm, context-motivated, structural-redesign, and parametric-design), and pairs it with an iteration message that carries the current program and its metrics.

ShinkaEvolve: full-rewrite format suffix

Rewrite the program to improve its performance on the specified metrics. Provide the complete new program code. You MUST respond using a short summary name, description and the full code:

<NAME>

A shortened name summarizing the code you are proposing. Lowercase, no spaces, underscores allowed.

</NAME>

<DESCRIPTION>

A description and argumentation process of the code you are proposing.

</DESCRIPTION>

<CODE>

```{language}

# The new rewritten program here.

```

</CODE>

* Keep the markers "EVOLVE-BLOCK-START" and "EVOLVE-BLOCK-END" in the code.

Do not change the code outside of these markers.

* Make sure your rewritten program maintains the same inputs and outputs as the original program, but with improved internal implementation.

* Make sure the file still runs after your changes.

* Use the <NAME>, <DESCRIPTION>, and <CODE> delimiters to structure your response. It will be parsed afterwards.

ShinkaEvolve: iteration message

Current program

Here is the current program we are trying to improve (you will need to propose a new program with the same inputs and outputs as the original program, but with improved internal implementation):

```{language}

{code\_content}

```

Here are the performance metrics of the program:

{performance_metrics}{text_feedback_section}

Task

Rewrite the program to improve its performance on the specified metrics. Provide the complete new program code.

IMPORTANT: Make sure your rewritten program maintains the same inputs and outputs as the original program, but with improved internal implementation.

ShinkaEvolve: CP system prompt

You are an expert computational geometer and optimization specialist focusing on circle-packing problems.

Your task is to improve a constructor function that arranges exactly 26 non-overlapping circles inside the unit square $[0,1] \times [0,1]$, maximizing the sum of their radii.

PROBLEM CONTEXT:

- Target: approach or beat the AlphaEvolve benchmark of `sum_radii = 2.635` for `n=26`
- Container: unit square with side length 1
- Constraints:
 - * All 26 circles must be fully contained in $[0,1] \times [0,1]$
 - * No two circles may overlap
 - * All radii must be positive and finite
- The metric is `combined_score = sum_radii / 2.635`

STRATEGIES TO CONSIDER:

- Hexagonal or honeycomb placement with edge-row adjustments
- Concentric shells or rings with varying radii
- Asymmetric layouts that exploit square-boundary effects
- Post-placement scaling so adjacent circles touch exactly
- Numerical refinement (`scipy.optimize`) on center positions after seeding a pattern

The evolve target is `construct_packing()`, which must return `(centers, radii, sum_radii)`, where `centers` has shape `(26, 2)`, `radii` has shape `(26,)`, and `sum_radii` is a scalar.

ShinkaEvolve: MMD system prompt

You are an expert computational geometer and optimization specialist focusing on point dispersion problems. Your task is to improve a constructor function that generates an optimal arrangement of exactly 16 points in 2D space, maximizing the ratio of minimum distance to maximum distance between all point pairs.

PROBLEM CONTEXT:

- Target: Beat the AlphaEvolve benchmark of min/max ratio $\approx 1/\sqrt{12.889266112} \approx 0.2786$
- Mathematical formulation: For points $P_i = (x_i, y_i)$, $i = 1, \dots, 16$:
 - * Distance matrix: $d_{ij} = \sqrt{(x_i - x_j)^2 + (y_i - y_j)^2}$ for all $i \neq j$
 - * Minimum distance: $d_{min} = \min\{d_{ij} : i \neq j\}$
 - * Maximum distance: $d_{max} = \max\{d_{ij} : i \neq j\}$
 - * Objective: maximize $(d_{min}/d_{max})^2$
- The metric is `inv_ratio_squared = (dmin/dmax)^2` and `combined_score = inv_ratio_squared / BENCHMARK`
- BENCHMARK = `1/12.889266112`

STRATEGIES TO CONSIDER:

- Regular polygon arrangements (vertices of regular n-gon)
- Multiple concentric rings of points
- Hexagonal lattice subsets
- Numerical optimization (`scipy.optimize`) to fine-tune positions

- Gradient descent on the min-distance objective

The function must be named `min_max_dist_dim2_16()` and return a numpy array

ShinkaEvolve: HT system prompt

You are an expert computational geometer and optimization specialist focusing on the Heilbronn triangle problem. Your task is to improve a constructor function that places exactly 11 points inside (or on the boundary of) an equilateral triangle with vertices $(0,0)$, $(1,0)$, and $(0.5, \sqrt{3}/2)$, so as to maximize the area of the smallest triangle formed by any three of the points.

PROBLEM CONTEXT:

- Target: approach or beat the AlphaEvolve benchmark of `min_area_normalized = 0.036529889880030156` for `n=11`
- Container: equilateral triangle with vertices $(0,0)$, $(1,0)$, $(0.5, \sqrt{3}/2)$. Its area is $\sqrt{3}/4$.
- Constraints:
 - * All 11 points must lie inside or on the boundary of the triangle (within tolerance $1e-6$)
 - * The objective is to maximize $\min\{ \text{area}(p_i, p_j, p_k) : 1 \leq i < j < k \leq 11 \}$
 - * The reported "min_area_normalized" is that minimum triangle area divided by the host triangle's area ($\sqrt{3}/4$)
- The metric is `combined_score = min_area_normalized / 0.036529889880030156`

CRITICAL - degeneracy warning:

- `combined_score = 0` if ANY three of the 11 points are collinear (the smallest triangle's area is then 0).
- Regular lattices, points along a triangle edge, and rotationally-symmetric grids almost always contain 3 collinear points and therefore score 0. Avoid them, or perturb them after seeding so no three points share a line.
- If you use a structured seed, follow it with numerical refinement (e.g. `scipy.optimize`) on the actual min-triangle-area (or a soft-min surrogate) to break collinearity.

The function must be named `heilbronn_triangle11()` and return a numpy array of shape `(11, 2)`.

I Use of AI Assistants

We used large language models (Anthropic's Claude) to assist with paper revising.

J Artifact Licenses

We use the following artifacts under their respective licenses, consistent with their intended research use:

- **OpenEvolve** (Apache-2.0): we use the example evaluators, initial programs, and prompt templates for Circle Packing, MinMaxDist, and Heilbronn Triangle verbatim.
- **Qwen3 1.7B / 4B / 8B / 14B** (Apache-2.0): used as the mutation engine in inference mode only; no weights modified.
- **Llama-3.1-8B** (Llama 3.1 Community License): used as the mutation engine in inference mode only; no weights modified.
- **vLLM** (Apache-2.0): used as the inference server.

K Ethics Statement

This work uses publicly available open-weight LLMs (Qwen3, Llama-3.1) and public geometric-optimization benchmarks. It involves no human subjects, no personal data, and no deployment in safety-critical settings. We foresee no direct ethical risks.

L Potential Risks

LLM-generated programs may contain correctness or security flaws that fitness-based evaluators do not catch, and adaptive allocation can concentrate compute on superficially promising trajectories.